CHAPTER IV

RESULTS AND DISCUSSION

4.1 Synthesis of dimethoxysaltrien metal complexes ($MSalOMe_2trien$)

Dimethoxysaltrien metal complexes ($MSalOMe_2trien$, where M = Zn and Ni) were synthesized following the synthetic route as described in the literature [30]. The reaction between 2-hydroxy-3-methoxybenzaldehyde and metal (II) acetate in methanol formed a template intermediate. Subsequently, the solution of triethylenetetramine was then added to obtain metal complexes ($MSalOMe_2$; M = Zn and Ni) as shown in Scheme 4.1.

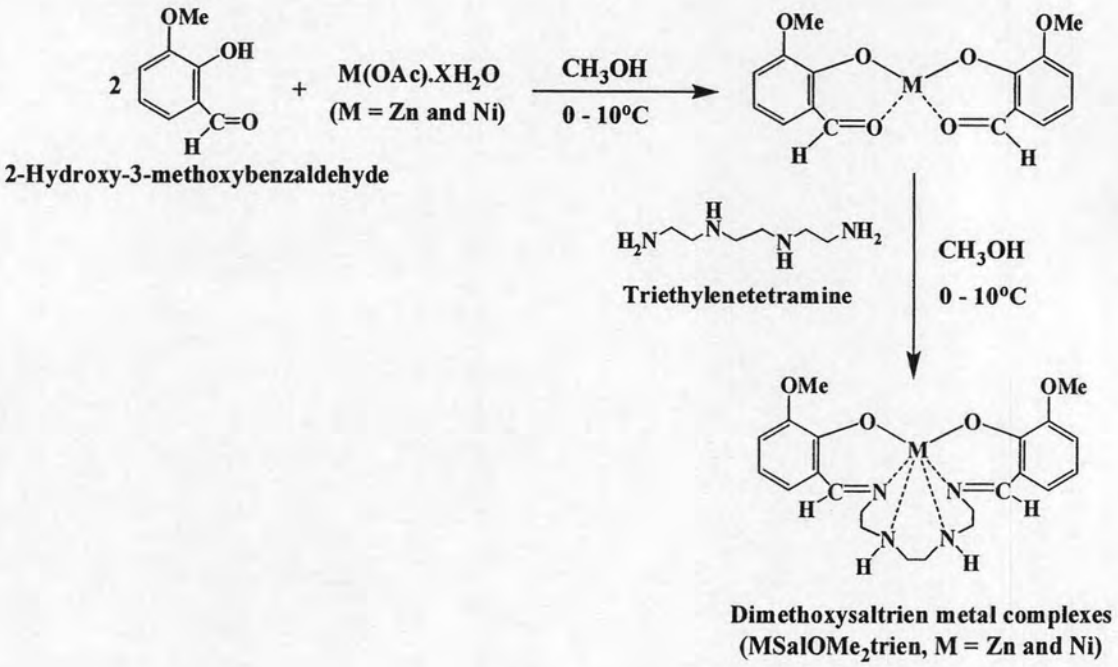

Scheme 4.1 Synthesis of dimethoxysaltrien metal complexes ($MSalOMe_2trien$)

The metal complexes were soluble in methanol, CH_2Cl_2 and acetone, partial soluble in DMF and insoluble in DMSO, hexane, tetrahydrofuran, water, acetonitrile and toluene.

4.1.1 Characterization of dimethoxysaltrien metal complexes (MSalOMe$_2$trien; M = Zn and Ni)

The obtained metal complexes were characterized by IR spectroscopy. The data agreed with those reported in the literature [30].

IR spectra of ZnSalOMe$_2$trien exhibited absorption bands of NH stretching at 3457-3310 cm^{-1}, C=N stretching at 1634 cm^{-1}, aromatic C=C stretching at 1597 cm^{-1} and aromatic C-O stretching at 1217 cm^{-1}. The bands at 973 and 789 cm^{-1} correspond to the characteristic absorption peak of aromatic bending of 1,2,3-trisubstituted benzene.

IR spectra of NiSalOMe$_2$trien exhibited absorption bands of NH stretching at 3438-3302 cm^{-1}, C=N stretching at 1633 cm^{-1}, aromatic C=C stretching at 1596 cm^{-1} and aromatic C-O stretching at 1217 cm^{-1}. The bands at 977 and 740 cm^{-1} correspond to the characteristic absorption peak of aromatic bending of 1,2,3-trisubstituted benzene.

^{1}H NMR data of ZnSalOMe$_2$trien also supported its structure as follows: δ 8.25 (2H, *s*, C**H**=N), 6.69 (2H, *dd*, Ar-**H**, *J* = 1.6, 8 Hz), 6.62 (2H, *dd*, Ar-**H**, *J* =1.6, 8 Hz), 6.14 (2H, *t*, Ar-**H**, *J* = 7.6 Hz), 3.84 -3.73 (2H, *m*, NC**H$_2$**), 3.59 (6H, *s*, OC**H$_3$**), 3.50-3.40 (2H, *m*, NC**H$_2$**), 3.22-2.99 (4H, *m*, HNC**H$_2$**), 2.84-2.71 (2H, *m*, HNC**H$_2$**), 2.40-2.28 (2H, *m*, HNC**H$_2$**).

4.2 Synthesis of metal-containing polyureas (MSalOMe$_2$trien-PUs)

4.2.1 Synthesis of MSalOMe$_2$trien-PUs from the reaction between MSalOMe$_2$trien and diisocyanates

Polyureas were synthesized by polyaddition reaction of MSalOMe$_2$trien with diisocyanates in both CH_2Cl_2 and DMF to study the solvent effect. DMF was used in the polymer synthesis since the copolymers, polyurethane-ureas and copolyureas, could not be synthesized in CH_2Cl_2. MSalOMe$_2$trien reacted with diisocyanates to give polyureas which immediately precipitated from the reaction mixture. Therefore, when dialcohols and diamines were added during the polymerization to yield polyurethane-ureas and polyureas, respectively, the precipitated polyureas could not undergo further reaction to give copolymers. MDI and HMDI were chosen as diisocyanates in the polymer synthesis. The polymerization was done in CH_2Cl_2 as described in the literature [30] (Scheme 4.2). The reaction was carried out at the mole ratio of MSalOMe$_2$trien:diisocyanate as 1:1 in CH_2Cl_2 and DMF for 12 hours. This research

used DMF to replace CH_2Cl_2. The yield of zinc and nickel-containing polyureas were 74-85% and 61-70%, respectively. Zinc and nickel-containing polyureas were obtained as yellow and light-green powder, respectively. The polyureas synthesized in DMF were compared with those synthesized in CH_2Cl_2.

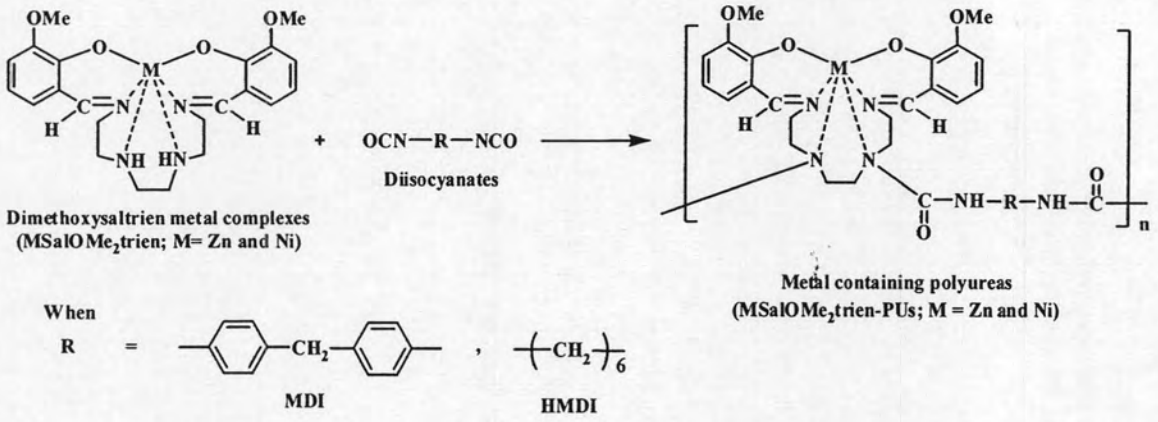

Scheme 4.2 Synthesis of $MSalOMe_2trien$-PUs from the reaction between $MSalOMe_2trien$ and diisocyanates [30]

The possible polymerization mechanism is that the amino groups in $MSalOMe_2trien$ undergo reaction with MDI (or HMDI) to give urea linkages (Scheme 4.3).

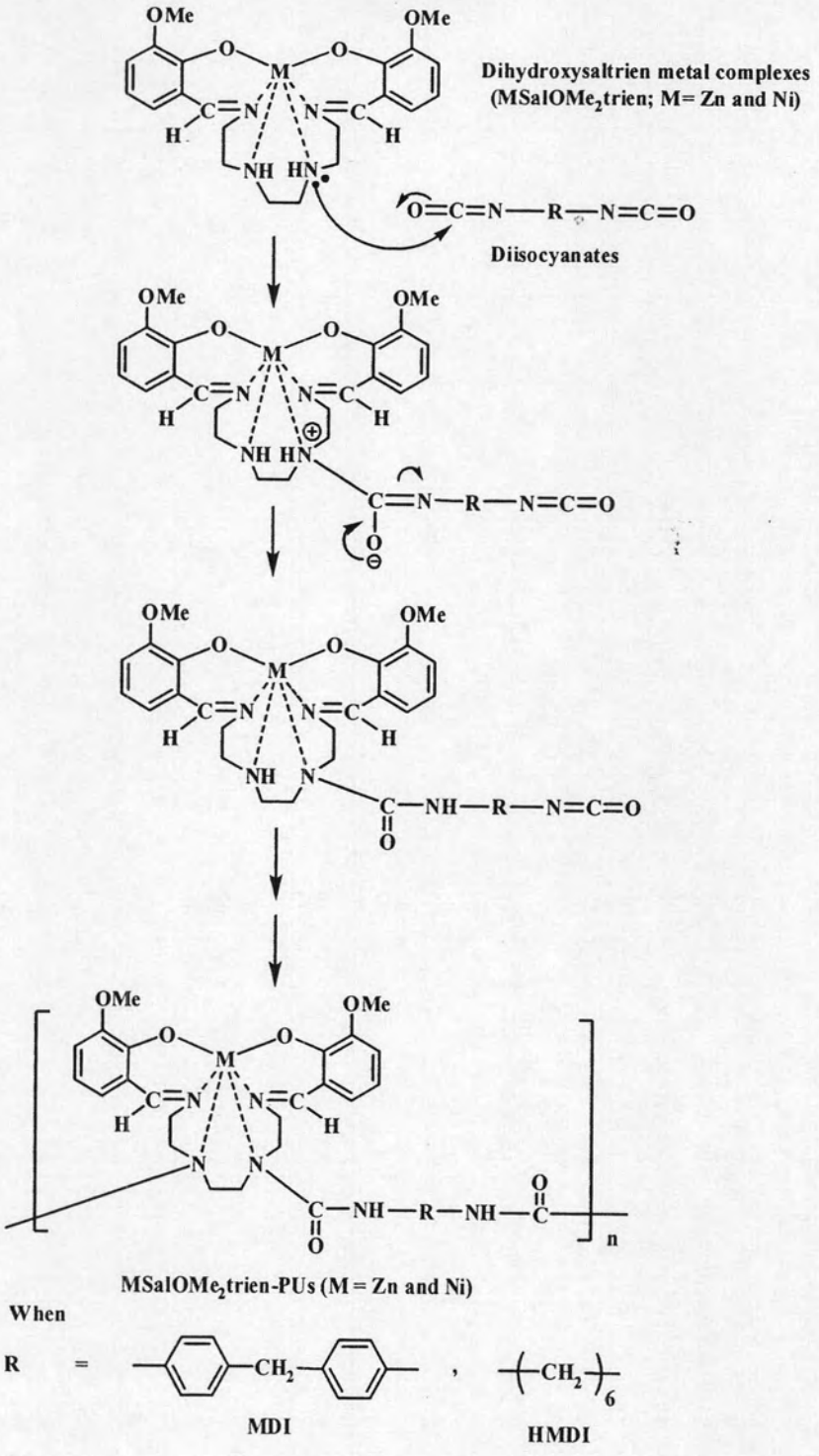

Scheme 4.3 Possible mechanism of the reaction between MSalOMe$_2$trien and MDI or HMDI

4.2.2 Characterization of MSalOMe$_2$trien-PUs

4.2.2.1 IR spectroscopy of MSalOMe$_2$trien-PUs

The FTIR spectra of zinc- and nickel-containing polyureas synthesized in DMF are displayed in Figures 4.1 shows IR absorption bands of the polymers. IR absorption bands of polyureas synthesized in DMF corresponded with those reported in the literature [30], which was synthesized in CH_2Cl_2. All of them showed N-H stretching signals of urea group in the region 3416-3331 cm^{-1}. The C-H stretching signals appeared between 2909-2931 cm^{-1} and the imine (C=N) absorption band was observed around 1628-1634 cm^{-1}. The carbonyl (C=O) stretching vibration of urea group (-NCON-) appeared as a broad peak due to the overlapping with -C=N- absorption.

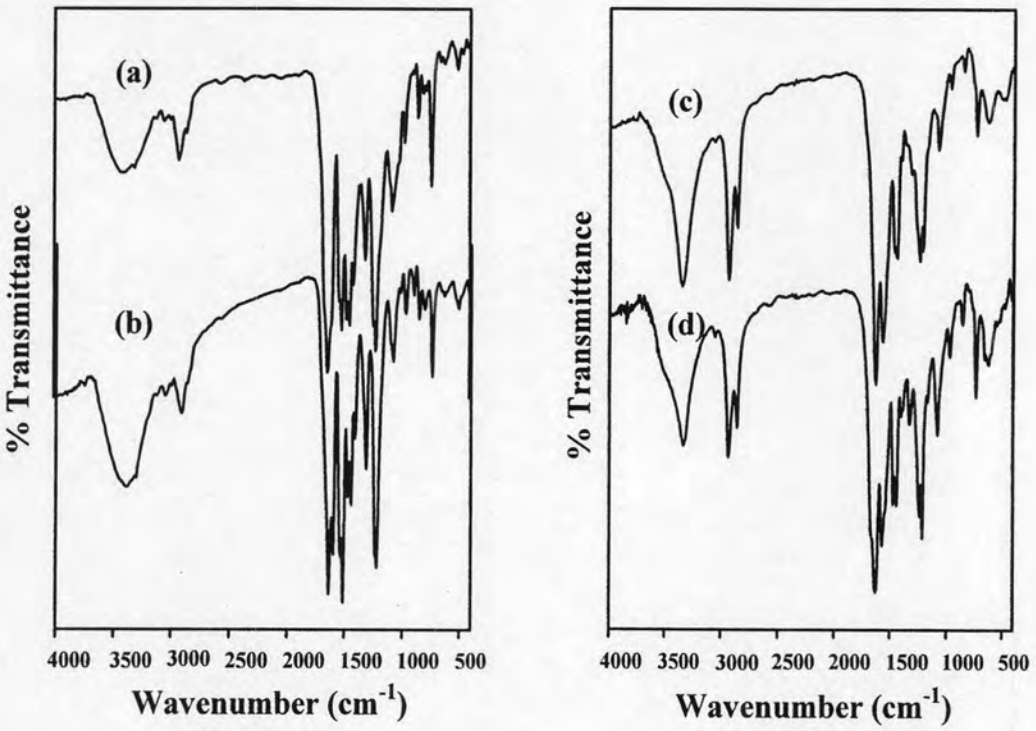

Figure 4.1 IR spectra of (a) ZnSalOMe$_2$trien-MDI; (b) NiSalOMe$_2$trien-MDI; (c) ZnSalOMe$_2$trien-HMDI; (d) NiSalOMe$_2$trien-HMDI

4.2.2.2 ^{1}H-NMR spectroscopy

^{1}H-NMR spectra of zinc-containing polyureas were recorded in DMSO-d_6 and their characteristic signals are presented in Figure 4.2 which corresponded with the data reported in the literature [30].

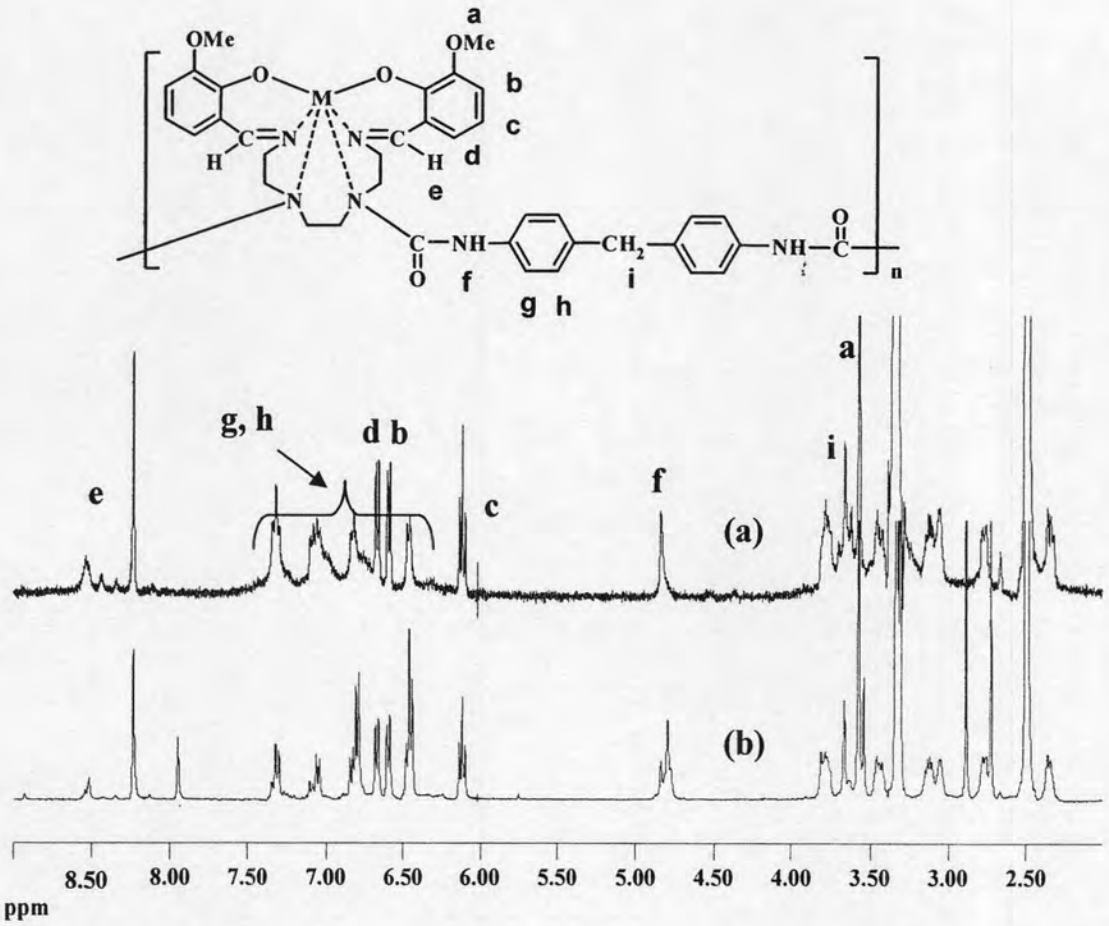

Figure 4.2 ^{1}H NMR spectrum of (a) ZnSalOMe$_2$trien-MDI obtained from CH_2Cl_2; (b) ZnSalOMe$_2$trien-MDI obtained from DMF

^{1}H-NMR spectra of ZnSalOMe$_2$trien-MDI obtained from CH_2Cl_2 and DMF showed similar pattern that the ratio of aromatic protons of ZnSalOMe$_2$trien:MDI was 6:8. The spectra showed the characteristic imine (-CH=N-) proton of ZnSalOMe$_2$trien at 8.24 ppm. The N-H signal of the urea group appeared at 4.90-4.72 ppm. The aromatic protons of ZnSalOMe$_2$trien showed signals at 6.71, 6.60 and 6.12 ppm whereas aromatic proton of MDI showed signals at 7.39-7.24, 7.15-6.99, 6.86-6.74, and 6.51-6.41 ppm.

4.2.2.3 Solubility

Solubility of metal containing polyureas was tested in various polar and non-polar solvents. The metal-containing polyureas synthesized in DMF showed that MDI-based polyureas were partially soluble DMSO after heating at 100°C for 12 hr. but insoluble in hexane, toluene, CH_3CN, H_2O, CH_2Cl_2, $CHCl_3$, MeOH, THF and DMF while HMDI-based polyureas were insoluble in all solvents. These solubility results were different from those of the polyureas synthesized in CH_2Cl_2 which were soluble in DMSO after heating for a few minute.

4.2.2.4 Inherent viscosity

Inherent viscosity of all polymers was measured at 40°C in DMSO as described in Appendix [B-1]. The viscosity data of metal-containing polyureas are given in Table 4.1. Zinc-containing polyureas showed lower viscosity than nickel-containing polyureas. Since the polyureas synthesized in DMF showed lower solubility in DMSO than those synthesized in CH_2Cl_2, the viscosity of MDI-based polymers were low and the viscosity of HMDI-based polymers could not be determined since the polymers were not completely soluble in DMSO.

Table 4.1 Inherent viscosity of metal-containing polyureas

Polymers	η_{inh} (dL/g)
Polymers synthesized in CH_2Cl_2 [30]	
ZnSalOMe$_2$trien-MDI	0.2428
ZnSalOMe$_2$trien-HMDI	0.1822
NiSalOMe$_2$trien-MDI	0.2198
NiSalOMe$_2$trien-HMDI	0.1212
Polymers synthesized in DMF	
ZnSalOMe$_2$trien-MDI	0.0588[a]
ZnSalOMe$_2$trien-HMDI	-
NiSalOMe$_2$trien-MDI	0.0821[a]
NiSalOMe$_2$trien-HMDI	-

[a] The polymer was completely soluble in DMSO after heating at 100°C for 12 hours

4.2.2.5 X-ray diffraction

The XRD patterns of metal-containing polyureas synthesized in DMF are presented in Figure 4.3. The XRD patterns revealed that all polymers were crystalline in nature. This XRD results corresponded with solubility results that the polyureas synthesized in DMF were partially soluble in hot DMSO.

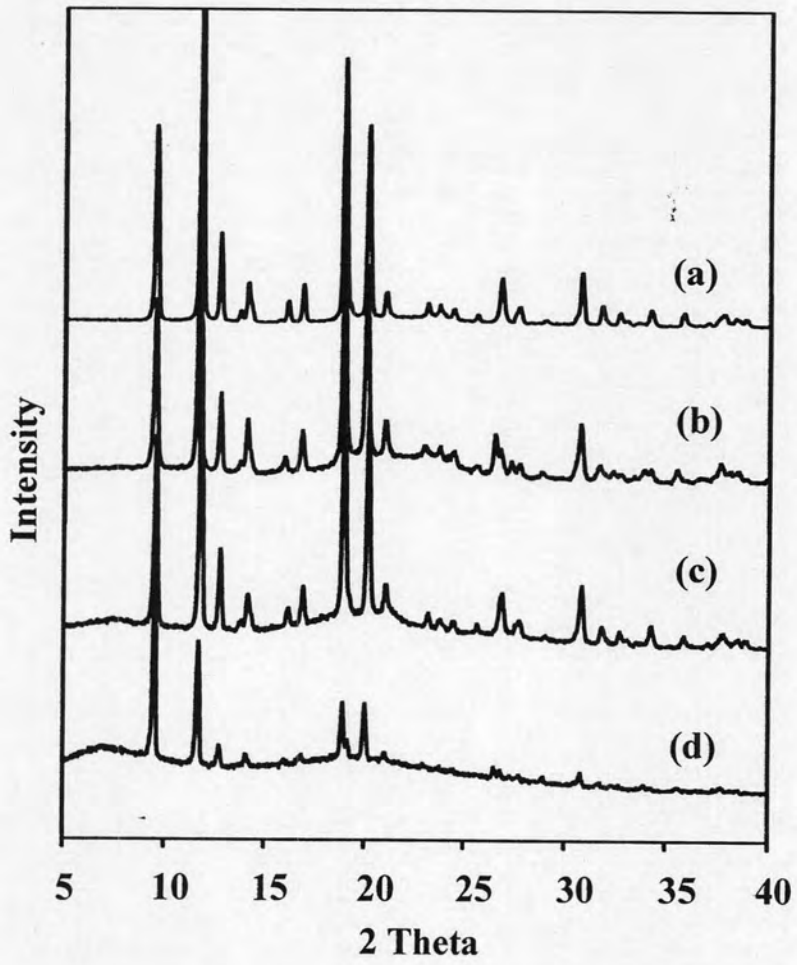

Figure 4.3 XRD patterns of (a) NiSalOMe$_2$trien-HMDI; (b) ZnSalOMe$_2$trien-HMDI; (c) ZnSalOMe$_2$trien-MDI; (d) NiSalOMe$_2$trien-MDI

4.2.2.6 Thermogravimetric analysis

TGA thermograms of metal-containing polyureas synthesized in DMF and weight loss data of metal-containing polyureas synthesized in CH_2Cl_2 and DMF are presented in Figure 4.4 and Table 4.2, respectively.

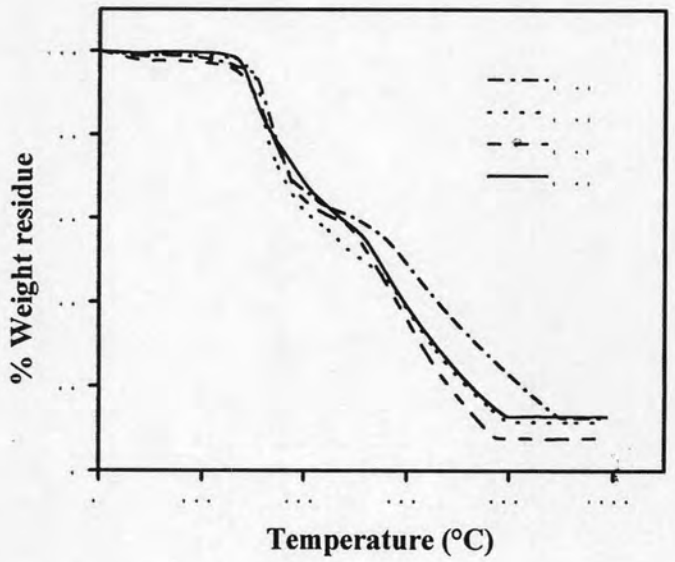

Figure 4.4 TGA thermograms of metal-containing polyureas synthesized in DMF (a) ZnSalOMe$_2$trien-MDI; (b) ZnSalOMe$_2$trien-HMDI; (c) NiSalOMe$_2$trien-MDI; (d) NiSalOMe$_2$trien-HMDI

Table 4.2 TGA data of zinc- and nickel-containing polyurethane-ureas

Polymer	T_5 (°C)	Weight loss (%) at different temperature (°C)						
		300	400	500	600	700	800	900
Polymers synthesized in CH_2Cl_2 [30]								
ZnSalOMe$_2$trien-MDI	226	21	32	41	56	70	81	85
ZnSalOMe$_2$trien-HMDI	220	11	36	42	57	73	84	87
NiSalOMe$_2$trien-MDI	190	11	44	51	65	81	89	89
NiSalOMe$_2$trien-HMDI	174	24	28	46	59	75	80	80
Polymers synthesized in DMF								
ZnSalOMe$_2$trien-MDI	295	6	34	40	51	65	77	88
ZnSalOMe$_2$trien-HMDI	294	6	31	49	62	78	89	89
NiSalOMe$_2$trien-MDI	268	10	36	44	64	83	92	92
NiSalOMe$_2$trien-HMDI	283	11	32	43	61	77	87	87

From TGA thermograms, the temperature at 5% weight loss (T_5) of metal-containing polymers synthesized in DMF was found to be in the range of 268-295°C which was higher than that of the polymers synthesized in CH_2Cl_2. The residual weights at 600°C were in the range of 36-49%. Zinc-containing polyureas showed higher thermal stability than nickel-containing polyureas. The polyureas synthesized in CH_2Cl_2 and DMF showed the same thermal stability at high temperature.

Possible mechanism of degradation proceeded *via* urea scission to give isocyanate and amine component (Scheme 4.4).

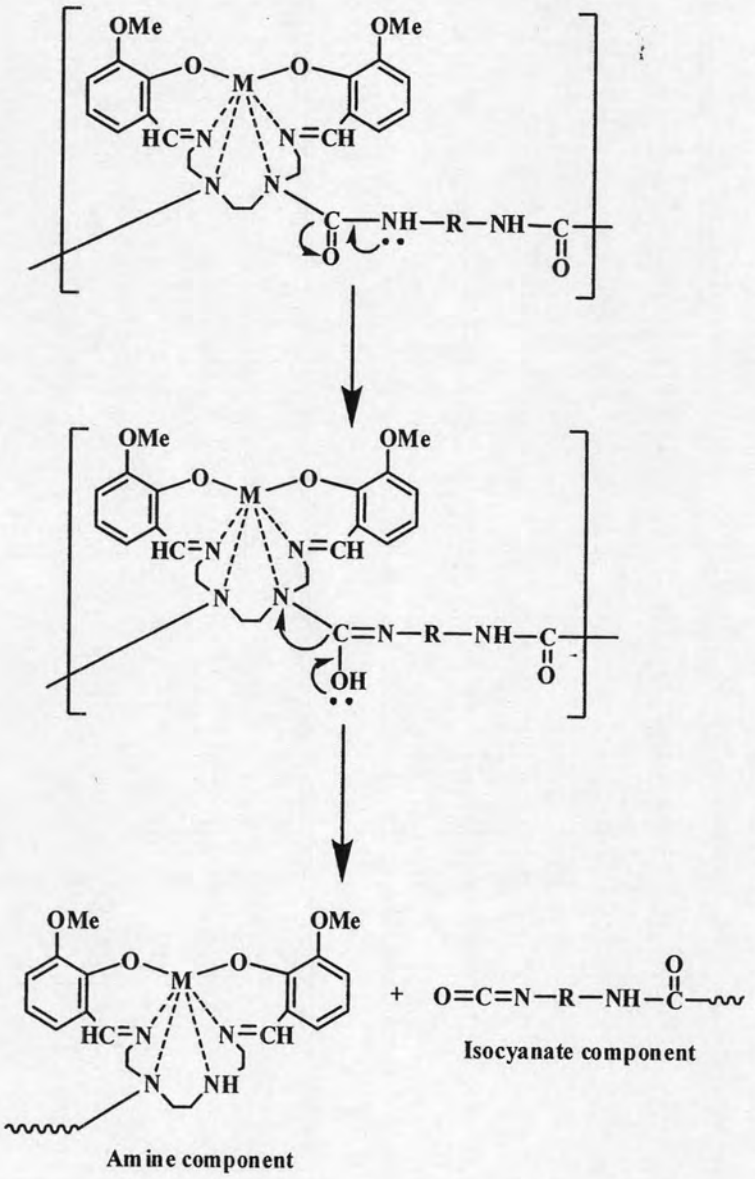

Scheme 4.4 Proposed mechanism of degradation of metal-containing polyureas

4.3 Synthesis of metal-containing polyurethane-ureas (MSalOMe$_2$trien-PUUs; M= Zn and Ni)

4.3.1 Synthesis of metal-containing polyurethane-ureas (MSalOMe$_2$trien-PUUs) from the reaction between MSalOMe$_2$trien, diisocyanates and dialcohols

The purpose of this work was to add urethane linkages into the polymer structure by addition of dialcohols during the polymerization. It was expected that this would improve solubility of the resulting polyurethane-ureas. Synthesis of polyurethane-ureas containing MSalOMe$_2$trien complexes (M = Zn and Ni) were done by the polyaddition reaction between MSalOMe$_2$trien, diisocyanates and dialcohols as shown in Schemes 4.5. The diisocyanates used were MDI and HMDI to obtain the polymers containing aromatic and aliphatic parts, respectively. Different dialcohols having aromatic, aliphatic and aliphatic ether groups were used to study effects on the polymer properties. The blank polyurethane-ureas without metal complexes were also prepared by the reaction of diisocyanates with dialcohols to study the influence of metal complexes on the thermal property of polymers.

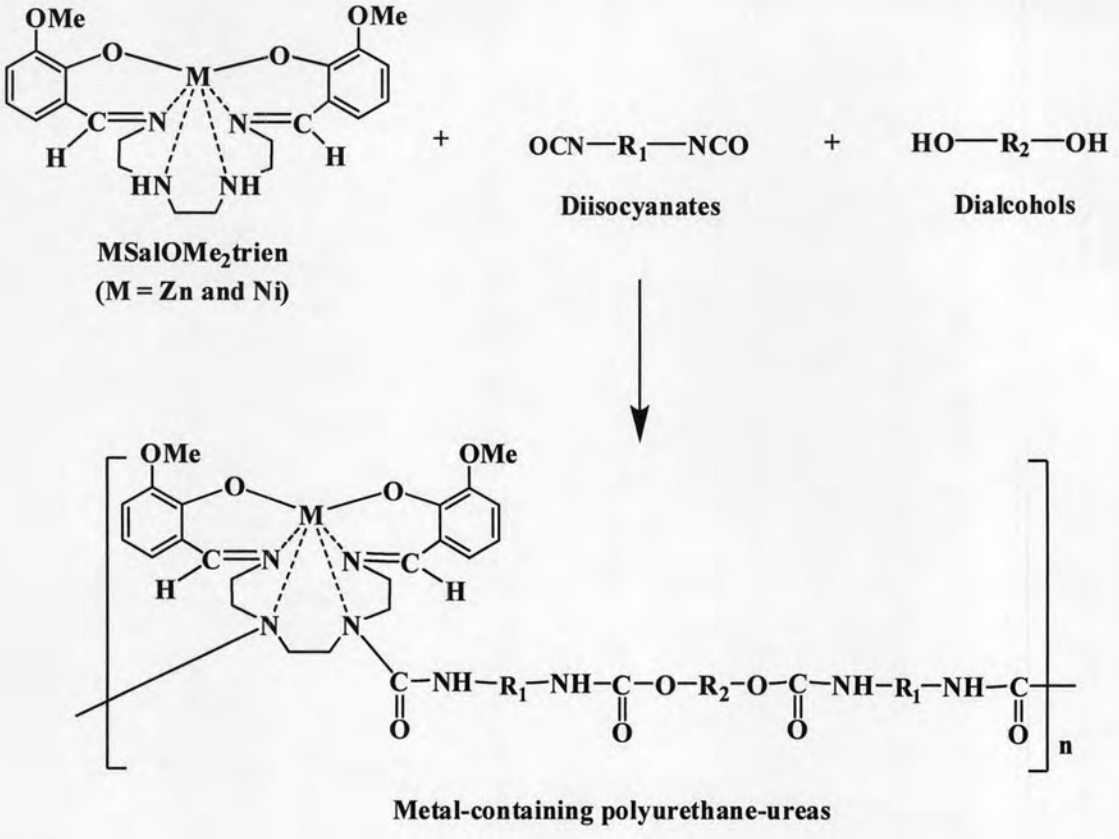

When

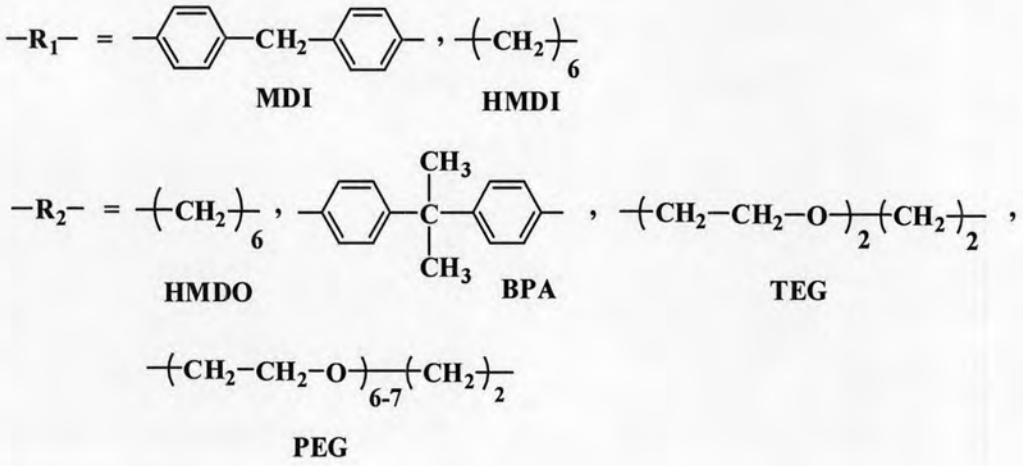

Scheme 4.5 Synthesis of MSalOMe$_2$trien-PUUs from the reaction between MSalOMe$_2$trien, diisocyanates and dialcohols

All metal-containing polyurethane-ureas were synthesized by taking the mole ratio of MSalOMe$_2$trien:diisocyanates:dialcohols as 1:2:1. Except for ZnSalOMe$_2$trien-MDI-PEG polyurethane-urea that was synthesized at the mole ratio 0.5:2:1.5, 1:2:1, and 1.5:2:0.5 to study the influence of metal complex content on properties of the polymers. It was expected that thermal stability of the polymer would

increase with increasing amount of metal complex. From TGA results, however, it was found that the composition of starting materials at the mole ratio of 1:2:1 gave the highest thermal stability (Figure 4.5 and Table 4.3). The temperature at 5% weight loss (T_5) of ZnSalOMe$_2$trien-MDI-PEG (1:2:1) was 293°C and the residual weight at 600°C was 64%. This result may be due to the steric hindrance in the metal complex structure. At the mole ratio of ZnSalOMe$_2$trien:MDI:PEG = 1.5:2:0.5, the metal complex could not undergo polymerization according to the expected mole ratio. Therefore, the thermal stability of ZnSalOMe$_2$trien:MDI:PEG (1.5:2:0.5) was lower than that of ZnSalOMe$_2$trien:MDI:PEG (1:2:1). Therefore, the composition of starting materials at the mole ratio of 1:2:1 was chosen for the synthesis of other polyurethane-ureas. The yields of metal-containing polyurethane-ureas and blank polyurethane-ureas were found to be in the ranges 54-96% and 25-97%, respectively (Table 4.4).

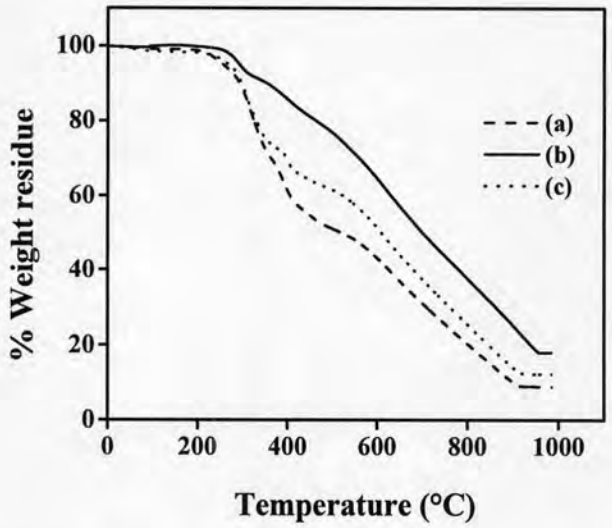

Figure 4.5 TGA thermogram of ZnSalOMe$_2$trien-MDI-PEG at the mole ratios of ZnSalOMe$_2$trien: MDI: PEG as (a) 0.5:2:1.5; (b) 1:2:1; (c) 1.5:2:0.5

Table 4.3 TGA data of ZnSalOMe$_2$trien-MDI-PEG

Polymer	T_5 (°C)	Weight loss (%) at different temperature (°C)						
		300	400	500	600	700	800	900
ZnSalOMe$_2$trien-MDI-PEG (1.5:2:0.5)	269	11	31	38	49	63	75	86
ZnSalOMe$_2$trien-MDI-PEG (1:2:1)	293	6	14	23	35	50	62	75
ZnSalOMe$_2$trien-MDI-PEG(0.5:2:01.5)	257	12	39	49	57	69	80	90

Table 4.4 Synthesis data of MSalOMe$_2$trien-PUUs and reference polyurethanes

Polymers	Yield (%)	External appearance
ZnSalOMe$_2$trien-MDI-HMDO	87	Yellow orange powder
ZnSalOMe$_2$trien-MDI-BPA	83	Orange brown powder
ZnSalOMe$_2$trien-MDI-TEG	69	Orange brown powder
ZnSalOMe$_2$trien-MDI-PEG (1.5:2:0.5)	62	Yellow brown powder
ZnSalOMe$_2$trien-MDI-PEG (1:2:1)	75	Yellow brown powder
ZnSalOMe$_2$trien-MDI-PEG (0.5:2:1.5)	54	Yellow orange powder
NiSalOMe$_2$trien-MDI-HMDO	91	Brown powder
NiSalOMe$_2$trien-MDI-BPA	92	Light brown powder
NiSalOMe$_2$trien-MDI-TEG	76	Dark brown powder
NiSalOMe$_2$trien-MDI-PEG	84	Red brown powder
ZnSalOMe$_2$trien-HMDI-HMDO	70	Red orange powder
ZnSalOMe$_2$trien-HMDI-BPA	88	Dark orange powder
ZnSalOMe$_2$trien-HMDI-TEG	75	Brown powder
ZnSalOMe$_2$trien-HMDI-PEG	54	Yellow orange powder
NiSalOMe$_2$trien-HMDI-HMDO	82	Dark brown powder
NiSalOMe$_2$trien-HMDI-BPA	92	Dark brown powder
NiSalOMe$_2$trien-HMDI-TEG	65	Dark brown powder
NiSalOMe$_2$trien-HMDI-PEG	56	Dark brown powder
MDI-HMDO	97	White powder
MDI-BPA	46	Light brown powder
MDI-TEG	85	Yellow powder
MDI-PEG	53	Yellow powder
HMDI-HMDO	38	White powder
HMDI-BPA	58	White powder
HMDI-TEG	41	White powder
HMDI-PEG	25	Yellow powder

The possible polymerization mechanism is proposed that the NH of metal complexes and OH of dialcohols undergo a reaction with isocyanate group to give urea and urethane linkages (Schemes 4.6).

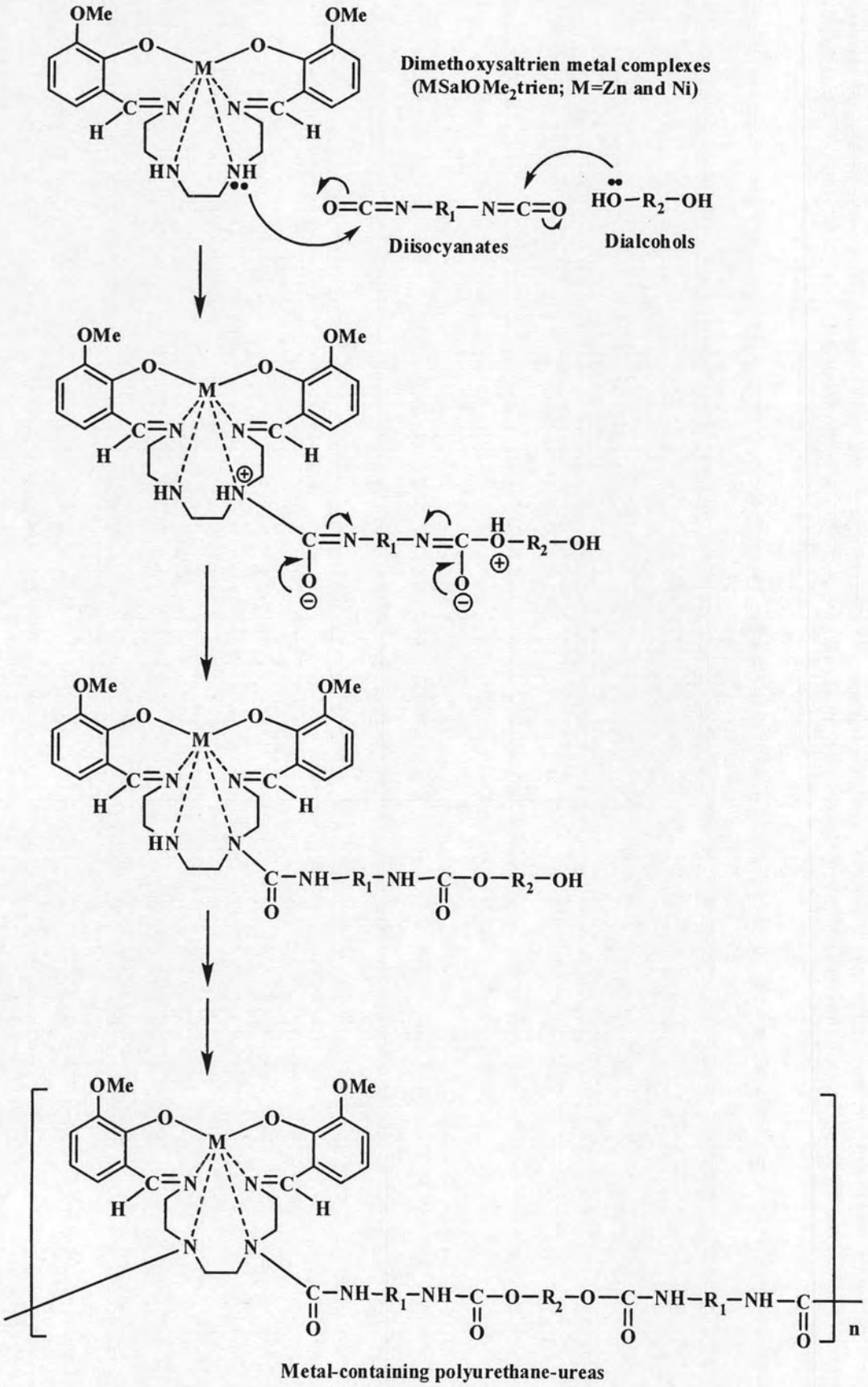

Scheme 4.6 Possible mechanism of the reaction between $MSalOMe_2trien$, diisocyanates and dialcohols to give polyurethane-ureas

4.3.1 Characterization of MSalOMe$_2$trien-containing PUUs

4.3.1.1 IR spectroscopy

IR spectra and data of the MSalOMe$_2$trien-containing PUUs are shown in Figures 4.6-4.7 and Tables 4.5-4.6, respectively. All metal-containing PUUs had similar IR absorption band. They showed a broad absorption band between 3426-3304 cm^{-1} that could be attributed to N-H stretching. The absorption bands at 2930-2852 cm^{-1} were due to the asymmetrical and symmetrical C-H stretching of methylene and methyl groups. The band around 1706-1697 cm^{-1} was attributed to the carbonyl stretching of urethane group (amide I). The peaks at 1633-1622 cm^{-1} were due to the imine (C=N) and carbonyl of urea group. The urethane carbonyl band in some metal-containing PUUs appeared as a shoulder or broad peak due to the overlapping with imine and urea carbonyl absorption. When the polymers was synthesized from the same MSalOMe$_2$trien and diisocyanate except different dialcohols were used, all BPA-based polymers showed broad band of urethane carbonyl stretching vibration overlapping with urea carbonyl and imine. This may be due to the resonance effect of aromatic ring of BPA that caused the urethane carbonyl peak to shift towards the lower wavenumber.

Figure 4.8 shows IR spectra of reference polyurethanes. The important characteristic absorption bands are as follows: 3336-3307 cm^{-1} (N-H stretching), 2966-2906 cm^{-1} (C-H stretching) and 1713-1692 cm^{-1} (C=O stretching of urethane).

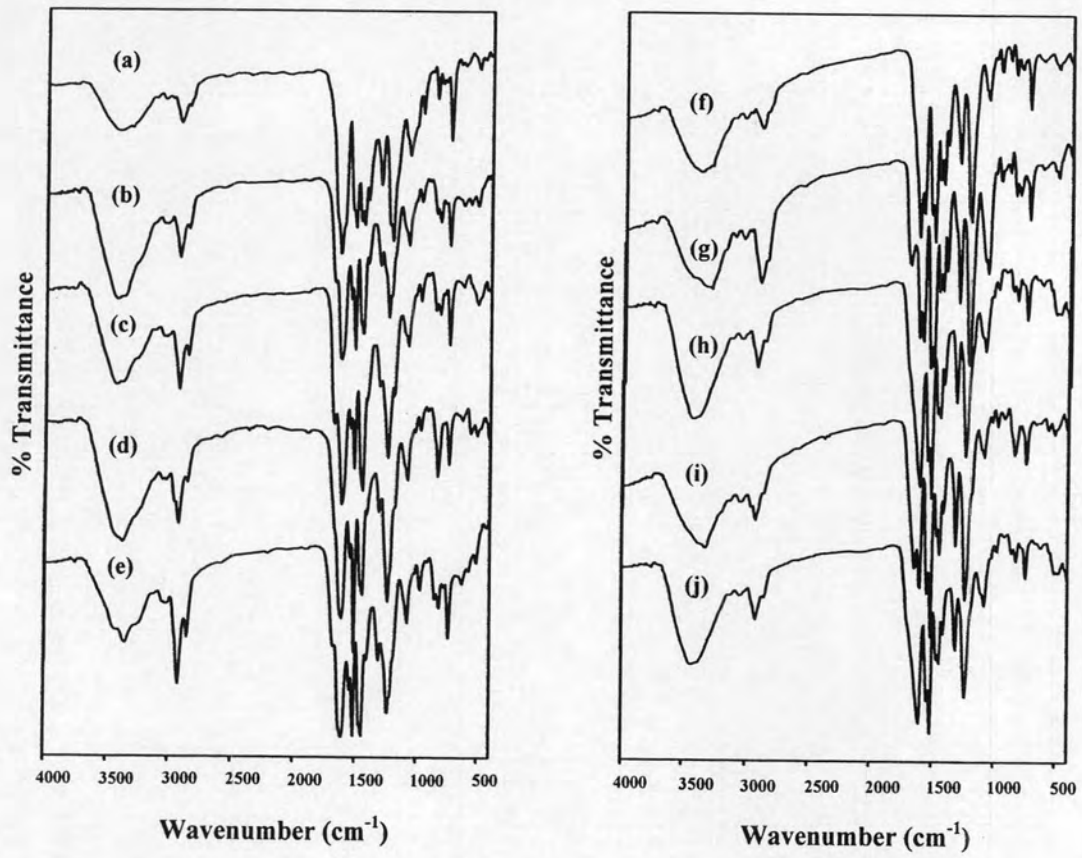

Figure 4.6 IR spectra of $MSalOMe_2trien$-containing PUUs

(a) $ZnSalOMe_2trien$-MDI; (b) $ZnSalOMe_2trien$-MDI-PEG;

(c) $ZnSalOMe_2trien$-MDI-TEG; (d) $ZnSalOMe_2trien$-MDI-BPA;

(e) $ZnSalOMe_2trien$-MDI-HMDO; (f) $NiSalOMe_2trien$-MDI;

(g) $NiSalOMe_2trien$-MDI-PEG; (h) $NiSalOMe_2trien$-MDI-TEG;

(i) $NiSalOMe_2trien$-MDI-BPA; (j) $NiSalOMe_2trien$-MDI-HMDO

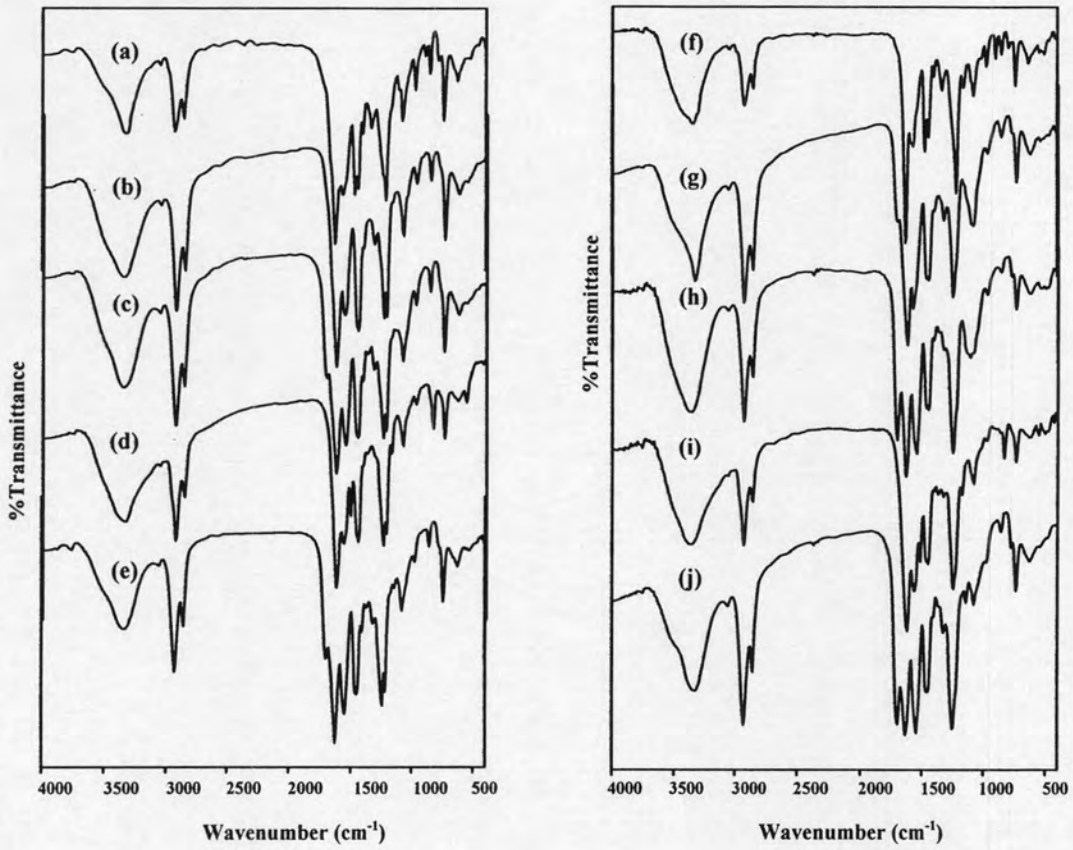

Figure 4.7 IR spectra of $MSalOMe_2trien$-containing PUUs

(a) $ZnSalOMe_2trien$-HMDI; (b) $ZnSalOMe_2trien$-HMDI-PEG;

(c) $ZnSalOMe_2trien$-HMDI-TEG; (d) $ZnSalOMe_2trien$-HMDI-BPA;

(e) $ZnSalOMe_2trien$-HMDI-HMDO; (f) $NiSalOMe_2trien$-HMDI;

(g) $NiSalOMe_2trien$-HMDI-PEG; (h) $NiSalOMe_2trien$-HMDI-TEG;

(i) $NiSalOMe_2trien$-HMDI-BPA; (j) $NiSalOMe_2trien$-HMDI-HMDO

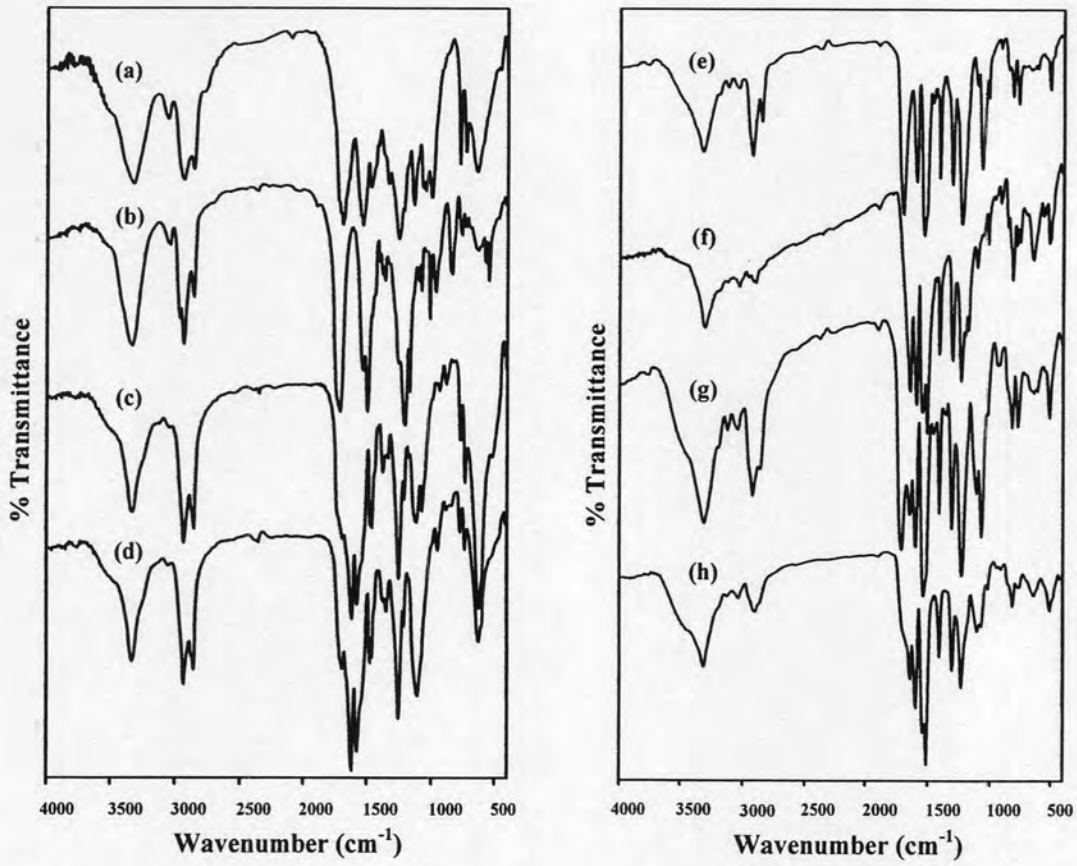

Figure 4.8 IR spectra of reference polyurethanes

(a) HMDI-HMDO; (b) HMDI-BPA; (c) HMDI-TEG; (d) HMDI-PEG;

(e) MDI-HMDO; (f) MDI-BPA; (g) MDI-TEG; (h) MDI-PEG

Table 4.5 IR assignment of Metal-containing PUUs based on MDI

Absorption band (cm^{-1}) [33]	Absorption band (cm^{-1}) [34]	Absorption band (cm^{-1})	Assignment [a]
3330-3060	3750-3050	3426-3304	N-H stretching vibration
2900-2800	3000-2800	2926-2852	CH_2 symmetric and antisymmetric stretching vibration
1750-1600	1800-1600	1706-1697	C=O stretching vibration of urethane group (amide I)
1640	-	1633-1622	C=N and C=O (urea group) stretching vibration
1800-1600, 1500-1400	-	1610-1600, 1515-1512	Aromatic ring stretching vibration
1570-1515	1589-1500	1543-1535	N-H bending (amide II) and C-N stretching vibration
-	1292-1200	1241-1225	In plane N-H and C-N stretching vibration (amide III)
1300-1100	-	1084-1075	C-O-C stretching vibration (ester, ether group)
900-800, 700-650	-	744-737	C-H out-of-plane deformation of 1,2,3-trisubstituted benzene

Table 4.6 IR assignment of Metal-containing PUUs based on HMDI

Absorption band (cm^{-1}) [33]	Absorption band (cm^{-1}) [34]	Absorption band (cm^{-1})	Assignment [a]
3330-3060	3750-3050	3362-3328	N-H stretching vibration
2900-2800	3000-2800	2930-2856	CH_2 symmetric and antisymmetric stretching vibration
1750-1600	1800-1600	1707-1677	C=O stretching vibration of urethane group (amide I)
1640	-	1641-1622	C=N and C=O (urea group) stretching vibration
1570-1515	1589-1500	1571-1545	N-H bending (amide II) and C-N stretching vibration
1800-1600, 1500-1400		1513-1512	Aromatic ring stretching vibration
-	1461-1453	1451-1444	CH_2 scissoring and CH_2 bending
-	1292-1200	1248-1242	In plane N-H and C-N stretching vibration (amide III)
1300-1100	-	1219-1107	C-O-C stretching vibration (ester, ether group)
900-800, 700-650		740-738	C-H out-of-plane deformation of 1,2,3-trisubstituted benzene

[a] The amide I mode is primary a C=O stretching band. The amide II mode is an out-of-phase combination of mostly N-H in plane bending and C-N stretching. Amide III mode is the in-phase combination of N-H in-plane bending and C-N stretching.

IR spectra of $MSalOMe_2trien$, $MSalOMe_2trien$-containing polyureas, $MSalOMe_2trien$-containing polyurethane-ureas and reference polyurethanes were compared as shown in Figures 4.9 and 4.10. It could be seen that $ZnSalOMe_2trien$-MDI-PEG, $NiSalOMe_2trien$-MDI-PEG and $NiSalOMe_2trien$-HMDI-PEG showed the urethane carbonyl absorption around 1706-1677 cm^{-1}. For $ZnSalOMe_2trien$-HMDI-PEG, its urethane carbonyl absorption was not clearly observed because it overlapped with imine and urea carbonyl peaks.

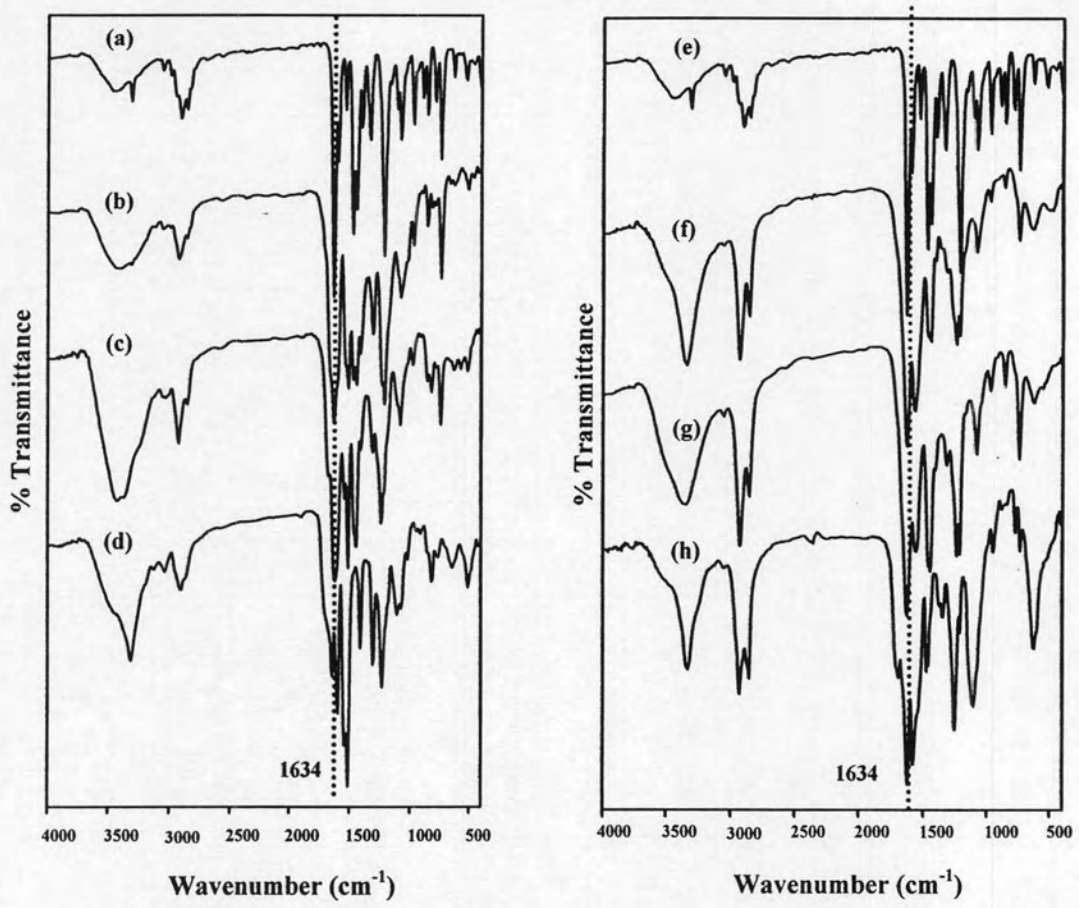

Figure 4.9 IR spectra of (a) $ZnSalOMe_2trien$; (b) $ZnSalOMe_2trien$-MDI; (c) $ZnSalOMe_2trien$-MDI-PEG; (d) MDI-PEG; (e) $ZnSalOMe_2trien$; (g) $ZnSalOMe_2trien$-HMDI; (g) $ZnSalOMe_2trien$-HMDI-PEG; (h) HMDI-PEG

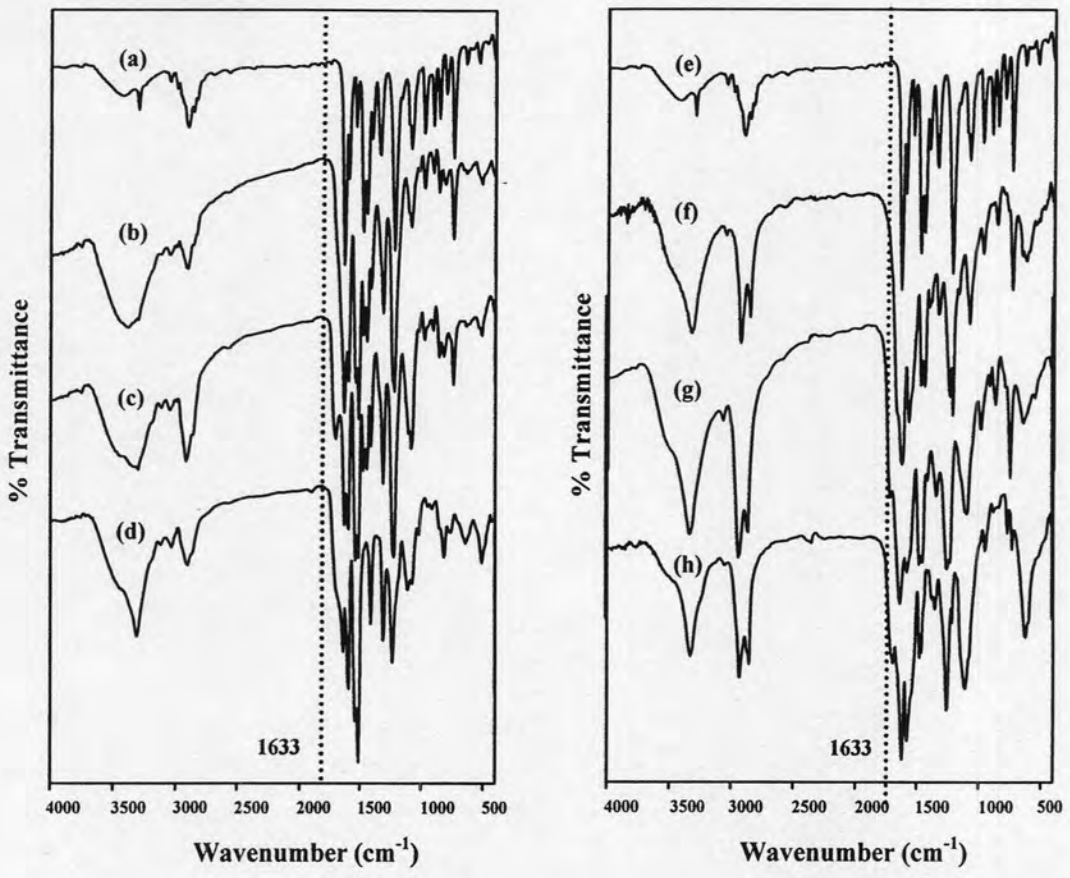

Figure 4.10 IR spectra of (a) NiSalOMe$_2$trien; (b) NiSalOMe$_2$trien-MDI; (c) NiSalOMe$_2$trien-MDI-PEG; (d) MDI-PEG; (e) NiSalOMe$_2$trien; (f) NiSalOMe$_2$trien-HMDI; (g) NiSalOMe$_2$trien-HMDI-PEG; (h) HMDI-PEG

IR spectra of ZnSalOMe$_2$trien-containing PUUs synthesized from the reaction between ZnSalOMe$_2$trien, MDI and PEG at different mole ratios of starting materials are shown in Figure 4.11. The spectra display the important peaks as follow: the peak at 1676 cm^{-1} is attributed to the carbonyl stretching of urethane group and the peaks at 1645-1633 cm^{-1} are due to the carbonyl stretching of urea group and C=N stretching of imine group. It was found that when the metal complex content in starting material composition decreased, the intensity of urea carbonyl and imine absorption decreased while the intensity of the urethane carbonyl increased.

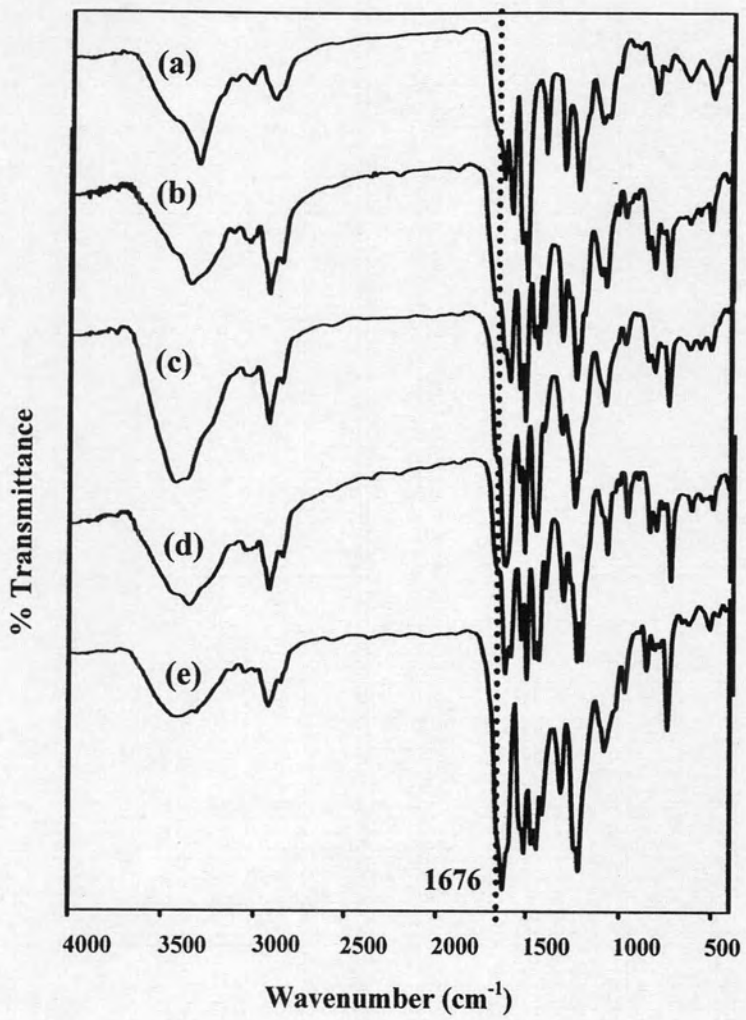

Figure 4.11 IR spectra of ZnSalOMe$_2$trien:MDI:PEG at the mole ratios of (a) 0:2:2; (b) 0.5:2:1.5; (c) 1:2:1; (d) 1.5:2:0.5; (e) 2:2:0

4.3.1.2 ^{1}H NMR spectroscopy

^{1}H NMR spectra and data of MSalOMe$_2$trien-containing polyurethane-ureas are shown in Figures 4.12-4.19 and Table 4.7. All of them showed the importance characteristic peaks as follows: CH=N and N-H protons of urethane group appeared at 9.21-6.94 and 4.66-4.14 ppm as multiplet and broad singlet peaks, respectively. The absorption of aromatic protons appeared in the range 7.57-5.85 ppm. N-H proton of urea group was observed at 5.83-4.67 ppm. The protons of methoxy, methylene attached to aromatic, and methylene group appeared in the range 4.20-1.06 ppm. Comparing between HMDI- and MDI-based metal-containing polyurethane-ureas, aromatic proton of MSalOMe$_2$trien in MDI-based polymers appeared as broad peaks so they overlapped with aromatic protons of MDI. ^{1}H NMR spectra of ZnSalOMe$_2$trien-MDI-PEG at the mole ratios of ZnSalOMe$_2$trien:MDI:PEG as 1.5:2:0.5, 1:2:1 and 0.5:2:1.5 are compared in Figure 4.18. The spectrum showed that the signals of ZnSalOMe$_2$trien increased when the content of ZnSalOMe$_2$trien was increased. The aromatic protons of ZnSalOMe$_2$trien were observed at 6.68, 6.60 and 6.12 ppm.

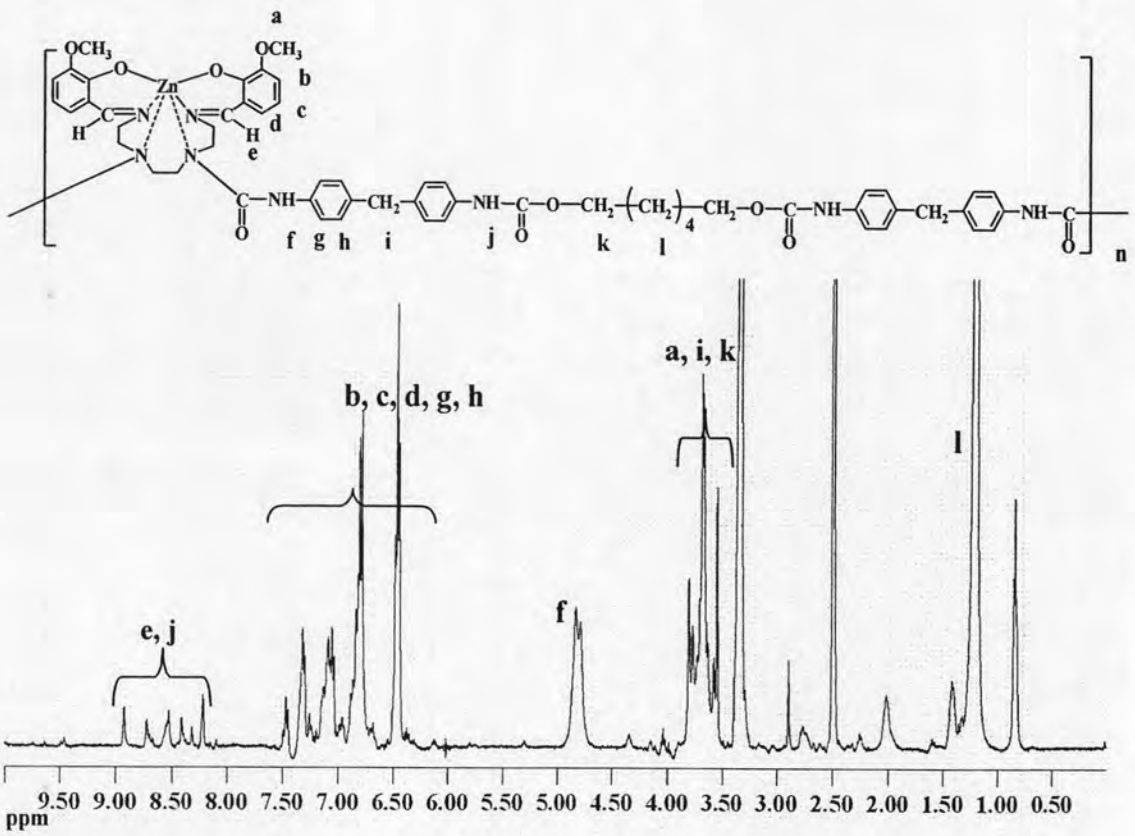

Figure 4.12 ^{1}H NMR spectrum of ZnSalOMe$_2$trien-MDI-HMDO in DMSO-d_6

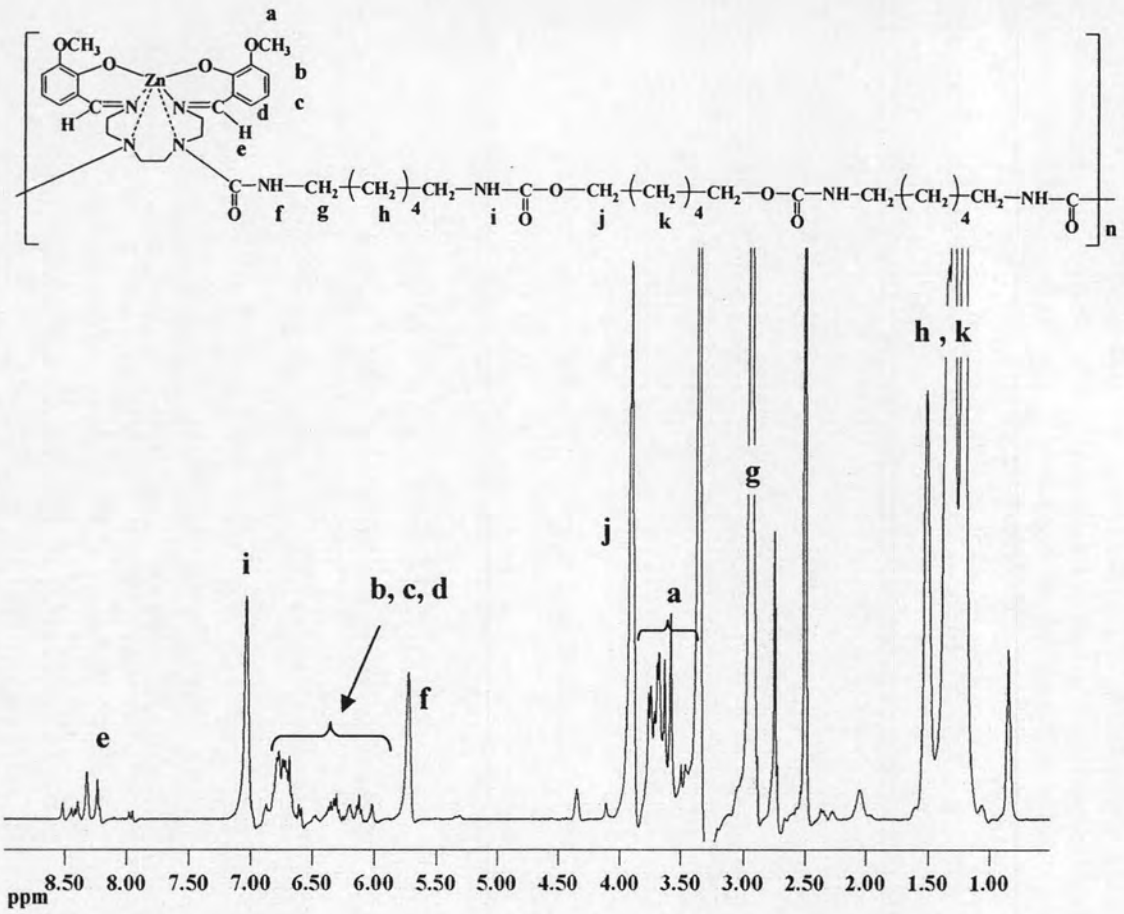

Figure 4.13 ^{1}H NMR spectrum of ZnSalOMe$_2$trien-HMDI-HMDO in DMSO-d_6

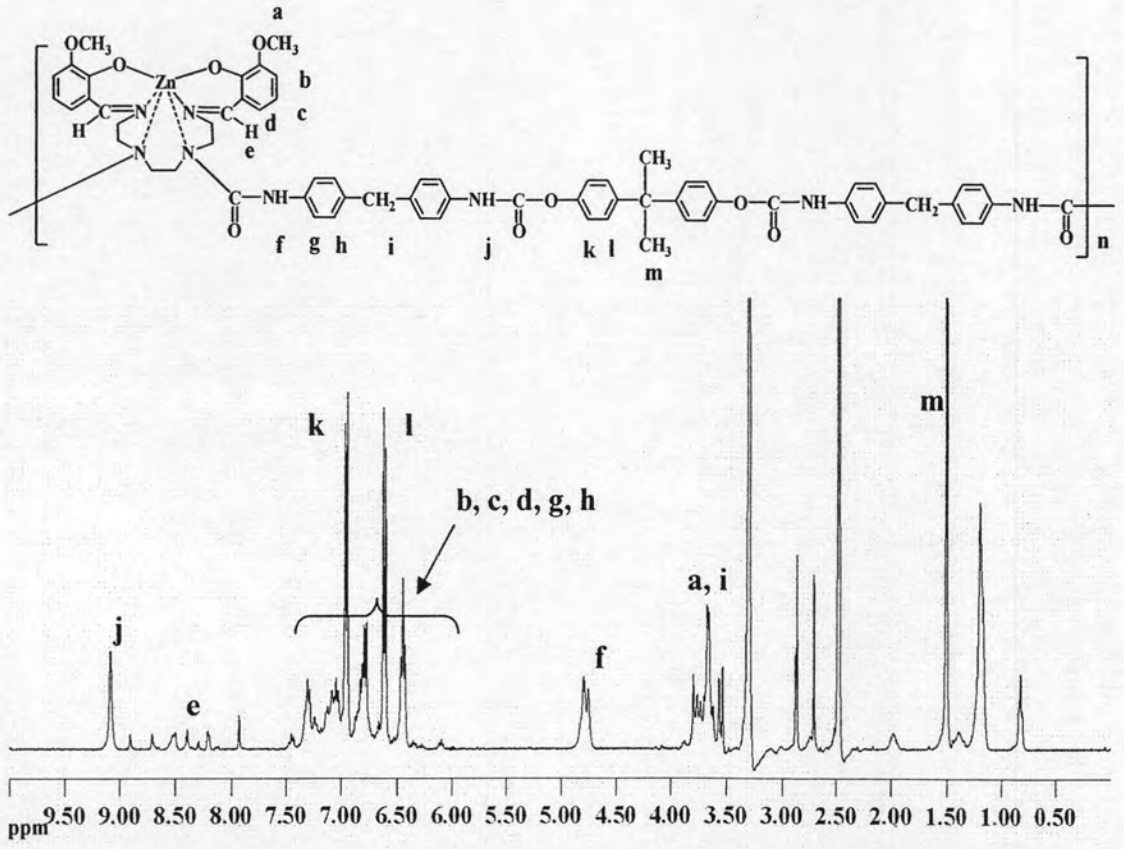

Figure 4.14 ^{1}H NMR spectrum of ZnSalOMe$_2$trien-MDI-BPA in DMSO-d_6

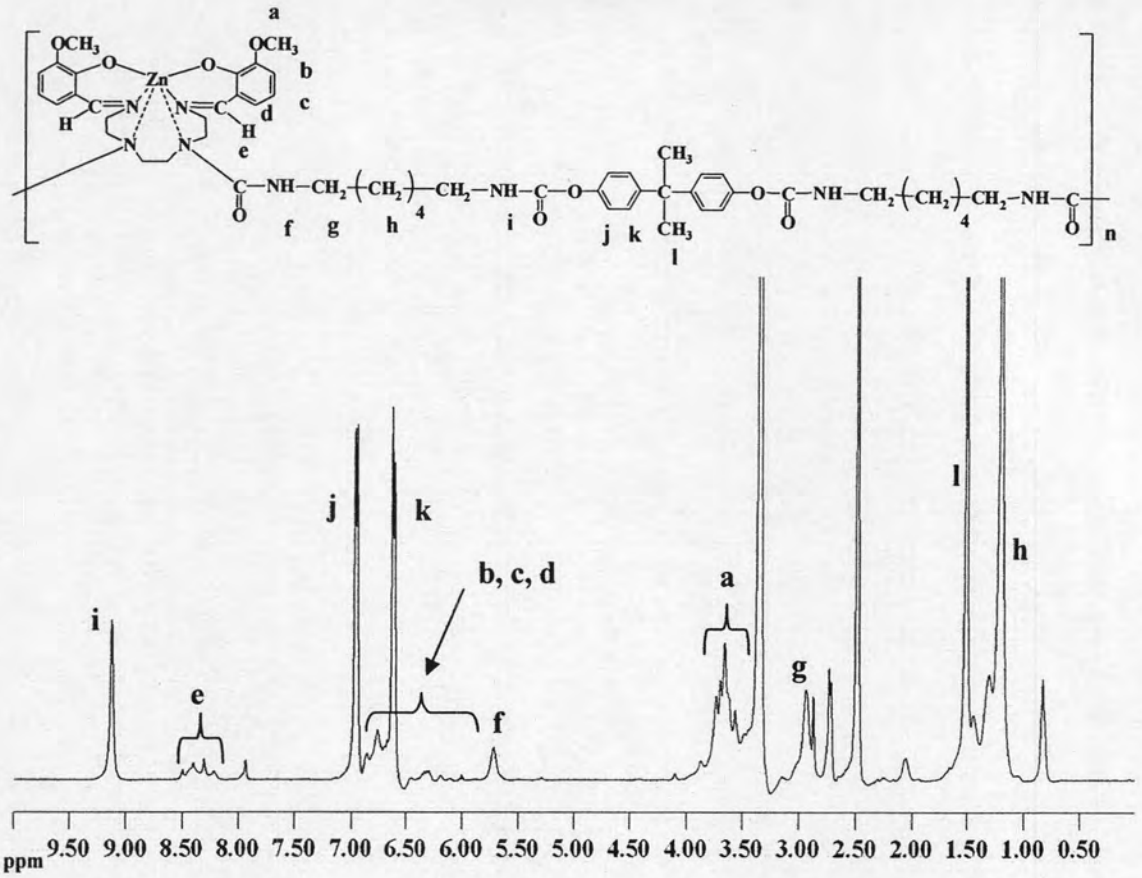

Figure 4.15 ^{1}H NMR spectrum of ZnSalOMe$_2$trien-HMDI-BPA in DMSO-d_6

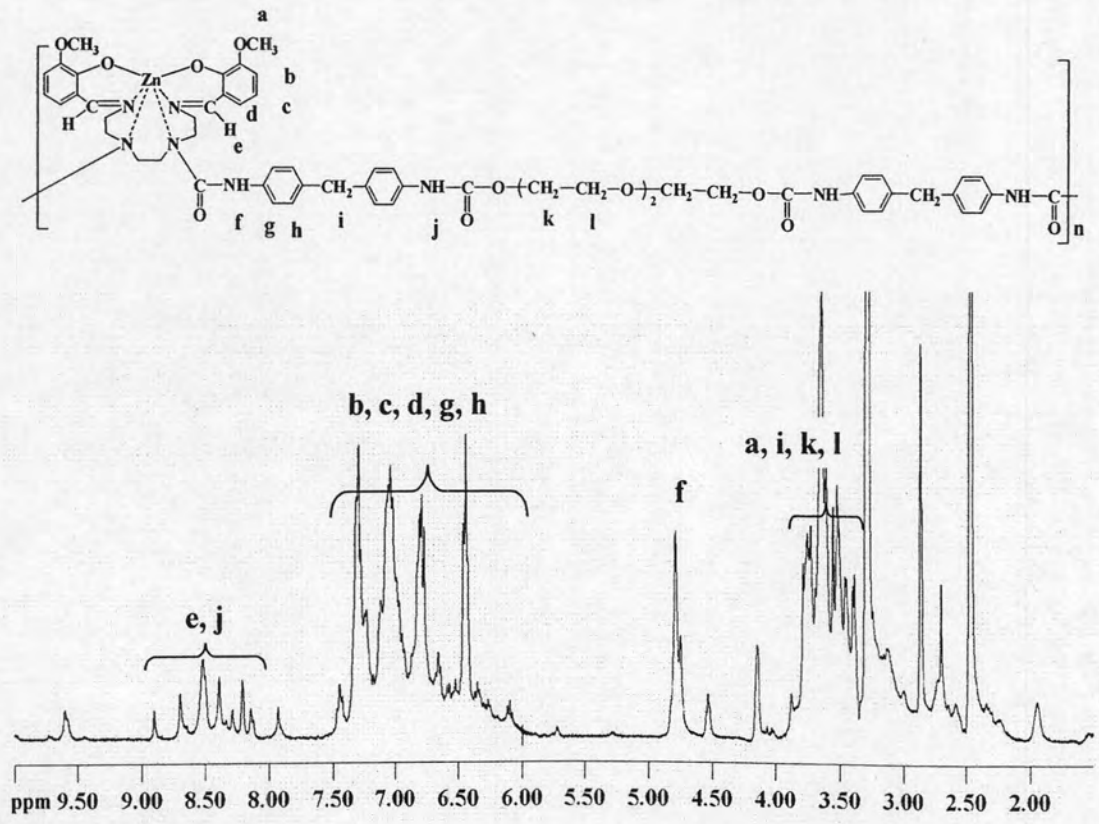

Figure 4.16 ^{1}H NMR spectrum of ZnSalOMe$_2$trien-MDI-TEG in DMSO-d_6

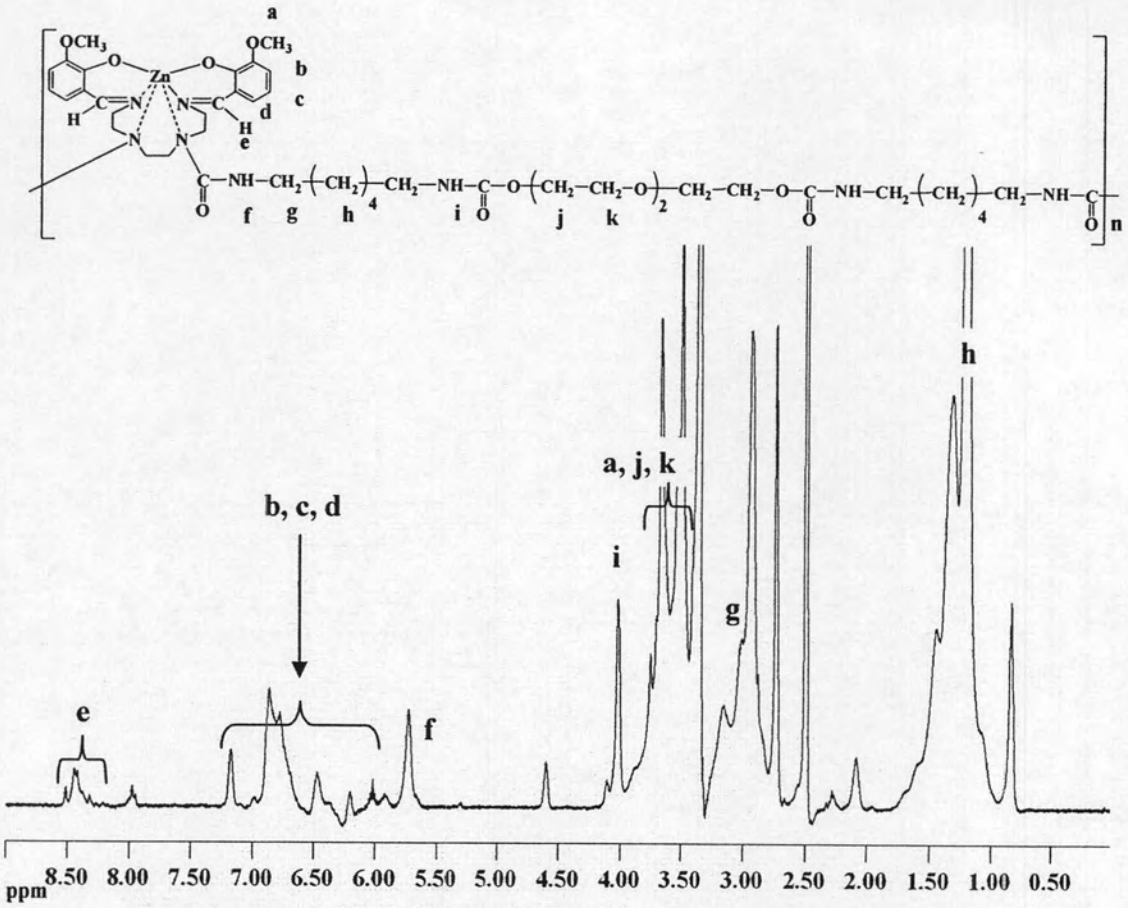

Figure 4.17 ^{1}H NMR spectrum of ZnSalOMe$_2$trien-HMDI-TEG in DMSO-d_6

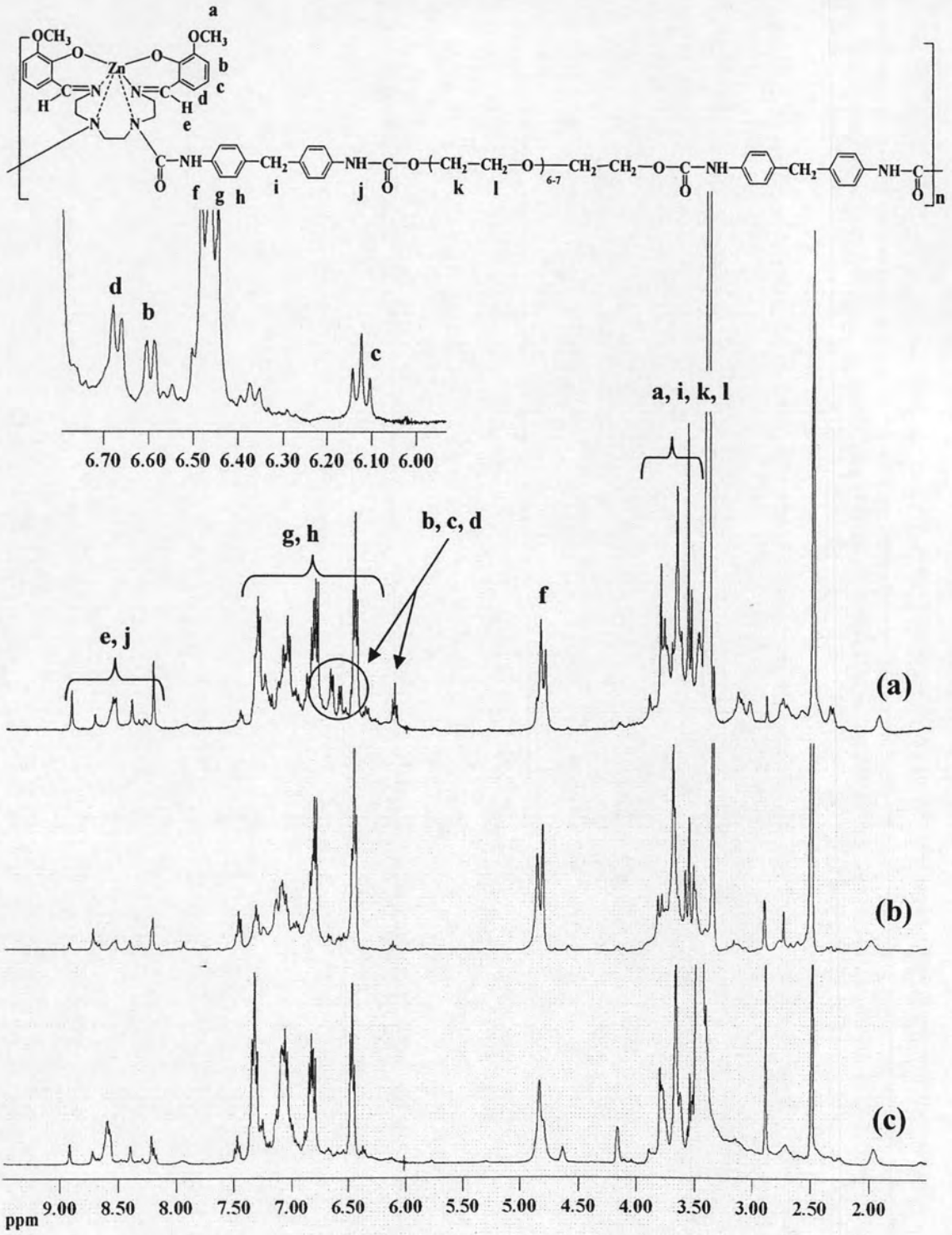

Figure 4.18 ^{1}H NMR spectra of ZnSalOMe$_2$trien-MDI-PEG at the mole ratios of ZnSalOMe$_2$trien:MDI:PEG as (a) 1.5:2:0.5; (b) 1:2:1; (c) 0.5:2:1.5

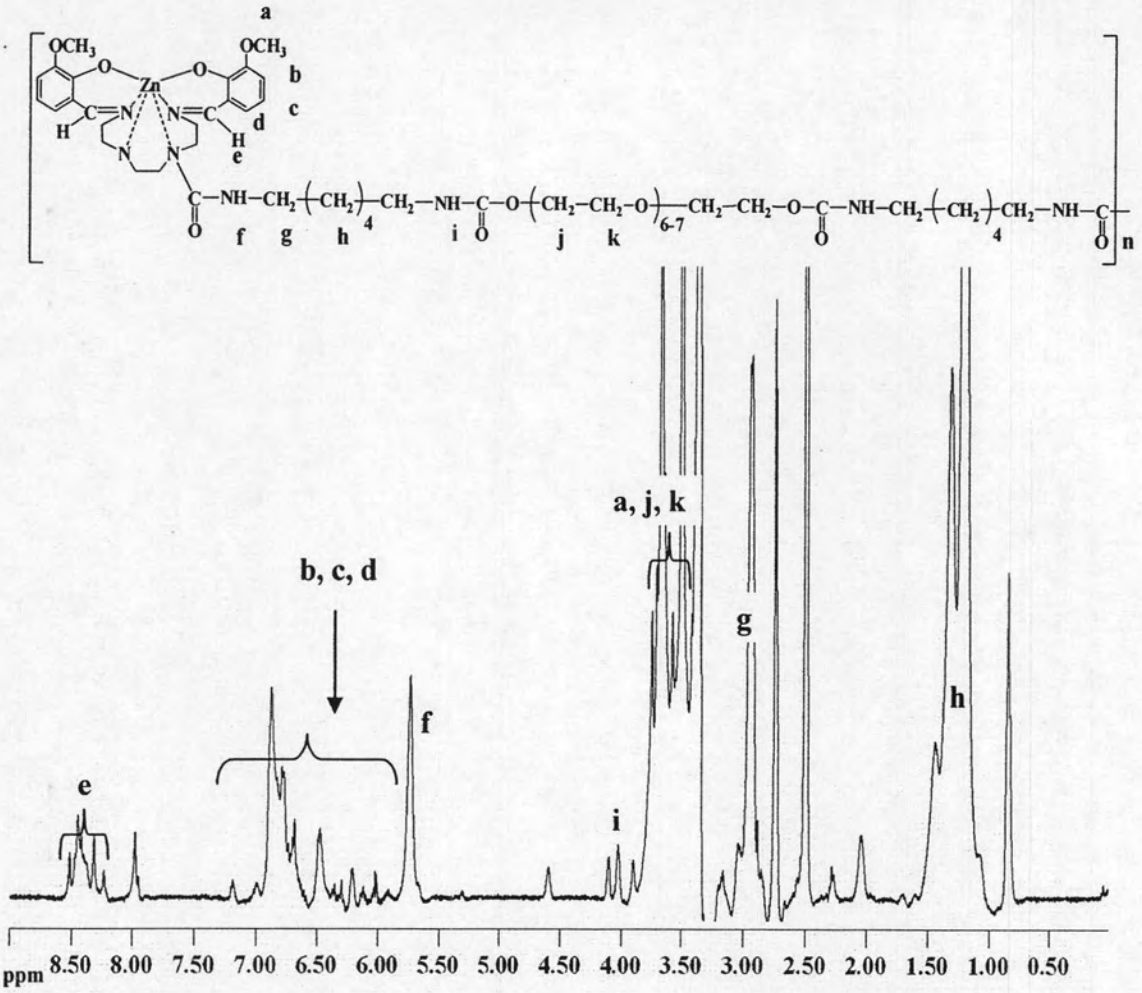

Figure 4.19 ^{1}H NMR spectrum of ZnSalOMe$_2$trien-HMDI-PEG in DMSO-d_6

Table 4.7 NMR assignment of MsalOMe$_2$trien-containing PUUs

Polyurethane-ureas	^{1}H NMR assignment
MDI-based polyurethane-ureas	
ZnSalOMe$_2$trien-MDI-HMDO	8.95-8.20 (*m*, C**H**=N and OC=ON**H**), 7.51-7.43 (*m*, Ar-**H**), 7.39-7.28 (*m*, Ar-**H**), 7.18-7.02 (*m*, Ar-**H**), 6.92-6.73 (*m*, Ar-**H**), 6.52-6.41 (*m*, Ar-**H**), 4.94-4.71 (*m*, NC=ON**H**), 3.85-3.76 (*m*, Ar-C**H**$_2$-Ar), 3.76-3.46 (*m*, OC**H**$_2$ and OC**H**$_3$), 1.48-1.07 (*m*, C**H**$_2$).
ZnSalOMe$_2$trien-MDI-BPA	9.15-9.02 (*brs*, OC=ON**H**), 8.94-7.89 (*m*, C**H**=N), 7.39-7.18 (*m*, Ar-**H**), 7.17-7.00 (*m*, Ar-**H**), 6.95 (*d*, *J* = 8.4 Hz, Ar-**H**), 6.93-6.73 (*m*, Ar-**H**), 6.61 (*d*, *J* = 8.4 Hz, Ar-**H**), 6.50-6.40 (*m*, Ar-**H**), 4.92-4.67 (*m*, NC=ON**H**), 3.86-3.48 (*m*, Ar-C**H**$_2$-Ar and OC**H**$_3$), 1.51 (*brs*, C**H**$_3$).
ZnSalOMe$_2$trien-MDI-TEG	8.95-7.88 (*m*, C**H**=N and OC=ON**H**), 7.57-7.17 (*m*, Ar-**H**), 7.17-6.91 (*m*, Ar-**H**), 6.89-6.62 (*m*, Ar-**H**), 6.61-6.23 (*m*, Ar-**H**), 4.88-4.69 (*m*, NC=ON**H**), 3.96-3.36 (*m*, OC**H**$_2$, OC**H**$_3$, and Ar-C**H**$_2$-Ar).
ZnSalOMe$_2$trien-MDI-PEG	8.98-8.19 (*m*, C**H**=N and OC=ON**H**), 7.53-7.42 (*m*, Ar-**H**), 7.42-7.21 (*m*, Ar-**H**), 7.21-6.93 (*m*, Ar-**H**), 6.93-6.74 (*m*, Ar-**H**), 6.70 (*d*, *J* = 7.6 Hz, Ar-**H**), 6.60 (*d*, *J* = 7.2 Hz, Ar-**H**), 6.51-6.41 (*m*, Ar-**H**), 6.10 (*t*, *J* = 7.6 Hz, Ar-**H**), 4.98-4.72 (*m*, NC=ON**H**), 4.20-3.43 (*m*, OC**H**$_2$, OC**H**$_3$, and Ar-C**H**$_2$-Ar).
HMDI-based polyurethane-ureas	
ZnSalOMe$_2$trien-HMDI-HMDO	8.56-7.90 (*m*, C**H**=N), 7.18-6.94 (*brs*, OC=ON**H**), 6.93-5.88 (*m*, Ar-**H**), 5.81-5.64 (*brs*, NC=ON**H**), 3.98-3.83 (*m*, HNCO-OC**H**$_2$), 3.84-3.53 (*m*, OC**H**$_3$), 3.01-2.86 (*m*, HN-C**H**$_2$), 1.64-1.09 (*m*, C**H**$_2$).

Table 4.7 NMR assignment of MsalOMe$_2$trien-containing PUUs (continued)

Polyurethane-ureas	^{1}H NMR assignment
ZnSalOMe$_2$trien-HMDI-BPA	9.21-9.04 (*brs*, OC=ON**H**), 8.54-7.87 (*m*, C**H**=N), 6.95 (*d*, *J* = 7.9 Hz, Ar-**H**), 6.90-6.66 (*m*, Ar-**H**), 6.61 (*d*, *J* = 7.9 Hz, Ar-**H**), 6.52-5.95 (*m*, Ar-**H**), 5.81-5.63 (*brs*, NC=ON**H**), 3.93-3.50 (*m*, O**CH$_3$**), 3.08-2.83 (*m*, HN-**CH$_2$**), 1.50 (*s*, **CH$_3$**), 1.38-1.06 (*brs*, **CH$_2$**).
ZnSalOMe$_2$trien-HMDI-TEG	8.56-7.90 (*m*, C**H**=N), 7.25-5.85 (*m*, Ar-**H**), 5.83-5.62 (*brs*, NC=ON**H**), 4.09-3.95 (*m*, OC=ON**H**), 3.82-3.44 (*m*, O**CH$_2$** and O**CH$_3$**), 3.10-2.84 (*m*, HN-**CH$_2$**), 1.51-1.10 (*m*, **CH$_2$**).
ZnSalOMe$_2$trien-HMDI-PEG	8.56-7.93 (*m*, C**H**=N), 7.24-5.89 (*m*, Ar-**H**), 5.81-5.66 (*brs*, NC=ON**H**), 4.14-3.86 (*m*, OC=ON**H**), 3.77-3.44 (*m*, O**CH$_2$** and O**CH$_3$**), 3.08-2.79 (*m*, HN-**CH$_2$**), 1.51-1.09 (*m*, **CH$_2$**).

4.3.1.3 Solubility

The solubility of metal-containing PUUs was tested in various polar and nonpolar solvents (Table 4.8 and 4.9). Solubility test showed that these metal-containing polymers were insoluble in hexane, toluene, CH_3CN, H_2O, CH_2Cl_2, $CHCl_3$, MeOH and THF. They were soluble in polar solvents such as DMF and DMSO. Metal-containing PUUs showed considerable better solubility than their corresponding metal-containing polyureas and reference polyurethanes synthesized without metal complexes.

Table 4.8 Solubility of MDI-based metal-containing polyureas, polyurethane-ureas and reference polyurethane

Polymers	DMF	Maximum solubility (mg)/ DMSO 1 mL
ZnSalOMe$_2$trien-MDI	-	5
NiSalOMe$_2$trien-MDI	-	5
ZnSalOMe$_2$trien-MDI-HMDO	++	1182
ZnSalOMe$_2$trien-MDI-BPA	++	1036
ZnSalOMe$_2$trien-MDI-TEG	++	1655
ZnSalOMe$_2$trien-MDI-PEG (1.5:2:0.5)	++	224
ZnSalOMe$_2$trien-MDI-PEG (1:2:1)	++	1089
ZnSalOMe$_2$trien-MDI-PEG (0.5:2:1.5)	++	753
NiSalOMe$_2$trien-MDI-HMDO	++	1339
NiSalOMe$_2$trien-MDI-BPA	++	435
NiSalOMe$_2$trien-MDI-TEG	++	1461
NiSalOMe$_2$trien-MDI-PEG	++	869
MDI-HDO	-	5
MDI-BPA	-	5
MDI-TEG	+	516
MDI-PEG	+	359

(-) Insoluble; (±) Partial soluble when heating; (+) Soluble when heating; (++) Good soluble at room temperature

Table 4.9 Solubility of HMDI-based metal-containing polyureas, polyurethane-ureas and reference polyurethane

Polymers	DMF	Maximum sulobility (mg)/ DMSO 1 mL
ZnSalOMe$_2$trien-HMDI	-	-
NiSalOMe$_2$trien-HMDI	-	-
ZnSalOMe$_2$trien-HMDI-HMDO	++	776
ZnSalOMe$_2$trien-HMDI-BPA	±	-
ZnSalOMe$_2$trien-HMDI-TEG	++	1061
ZnSalOMe$_2$trien-HMDI-PEG	++	419
NiSalOMe$_2$trien-HMDI-HMDO	++	280
NiSalOMe$_2$trien-HMDI-BPA	-	-
NiSalOMe$_2$trien-HMDI-TEG	++	372
NiSalOMe$_2$trien-HMDI-PEG	-	-
HMDI-HDO	-	-
HMDI-BPA	-	-
HMDI-TEG	-	-
HMDI-PEG	-	-

(-) Insoluble; (±) Partial soluble when heating; (+) Soluble when heating; (++) Good soluble at room temperature

The maximum amount of each polymer that was able to dissolve in 1 mL of DMSO was determined as shown in Tables 4.8 and 4.9. Most zinc-containing PUUs showed higher solubility than nickel-containing PUUs. The solubility of ZnSalOMe$_2$trien-MDI-PEG polymer at the various mole ratios exhibited that ZnSalOMe$_2$trien:MDI:PEG (1:2:1) had the highest solubility. HMDI-based metal-containing PUUs exhibited lower solubility than MDI-based metal-containing PUUs because they were partially crystalline in nature from the folding of the hexamethylene groups [35-38]. The comparison between metal-containing PUUs synthesized from the same metal complex and diisocyanate showed that TEG-based metal-containing PUUs had better solubility than HMDO, PEG and BPA-based polymers. This might be because TEG has flexible ether bonds. Most of metal-containing PUUs were more soluble in DMSO as compared to metal-containing polyureas. These results were comfirmed with XRD data of the polymers.

4.3.1.4 Inherent viscosity

The inherent viscosity of metal-containing PUUs and reference polyurethanes was measured at a concentration 0.5 g/ 100 mL in DMSO 40 °C. The viscosity data are shown in Table 4.10.

Table 4.10 Inherent viscosity of metal-containing polyureas, polyurethane-ureas and reference polyurethane

Polymers	η_{inh} (dL/g)
ZnSalOMe$_2$trien-MDI-HDO	0.0891
ZnSalOMe$_2$trien-MDI-BPA	0.0805
ZnSalOMe$_2$trien-MDI-TEG	0.0797
ZnSalOMe$_2$trien-MDI-PEG (1.5:2:0.5)	0.0931
ZnSalOMe$_2$trien-MDI-PEG (1:2:1)	0.0955
ZnSalOMe$_2$trien-MDI-PEG (0.5:2:1.5)	0.1014
NiSalOMe$_2$trien-MDI-HDO	0.0962
NiSalOMe$_2$trien-MDI-BPA	0.1004
NiSalOMe$_2$trien-MDI-TEG	0.0887
NiSalOMe$_2$trien-MDI-PEG	0.1095
MDI-HDO (1:1)	0.1107
MDI-BPA (1:1)	0.0961
MDI-TEG (1:1)	0.1065
MDI-PEG (1:1)	0.1306
ZnSalOMe$_2$trien-HMDI-HDO	0.0801
ZnSalOMe$_2$trien-HMDI-BPA	-
ZnSalOMe$_2$trien-HMDI-TEG	0.0808
ZnSalOMe$_2$trien-HMDI-PEG	0.0845
NiSalOMe$_2$trien-HMDI-HDO (1:2:1)	0.0927
NiSalOMe$_2$trien-HMDI-BPA (1:2:1)	-
NiSalOMe$_2$trien-HMDI-TEG (1:2:1)	0.1041
NiSalOMe$_2$trien-HMDI-PEG (1:2:1)	-
HMDI-HDO (1:1)	-
HMDI-BPA (1:1)	-
HMDI-TEG (1:1)	-
HMDI-PEG (1:1)	-

The data showed that the inherent viscosity of the metal-containing PUUs was found to be in the range between 0.0797-0.1095 dl/g. The viscosity of metal-containing PUUs was lower than reference polyurethanes without metal complexes in both Zn and Ni series.

4.3.1.5 X-ray diffraction

The XRD patterns of ZnSalOMe$_2$trien-MDI-TEG, ZnSalOMe$_2$trien-MDI-PEG, NiSalOMe$_2$trien-MDI-TEG, and NiSalOMe$_2$trien-MDI-PEG were shown in Figure 4.20. The only XRD pattern of NiSalOMe$_2$trien-MDI-PEG showed sharp peaks while another showed broad peaks so the polymers were considered to be semi-crystalline and amorphous in nature, respectively. The amorphous property of polymers was supported by the solubility test of polymers which showed that the ZnSalOMe$_2$trien-MDI-TEG, ZnSalOMe$_2$trien-MDI-PEG, and NiSalOMe$_2$trien-MDI-TEG were soluble in DMF and DMSO and the solution was clear. The solution of NiSalOMe$_2$trien-MDI-PEG in DMF and DMSO was hazy so the polymer was considered as semi-crystalline. Comparing between ZnSalOMe$_2$trien-MDI-PEG at different ratios, the XRD patterns showed that the polymers were amorphous in nature. Sharp peak at 2θ = 6-7 disappeared when the amount of ZnSalOMe$_2$trien decreased (Figure 4.21).

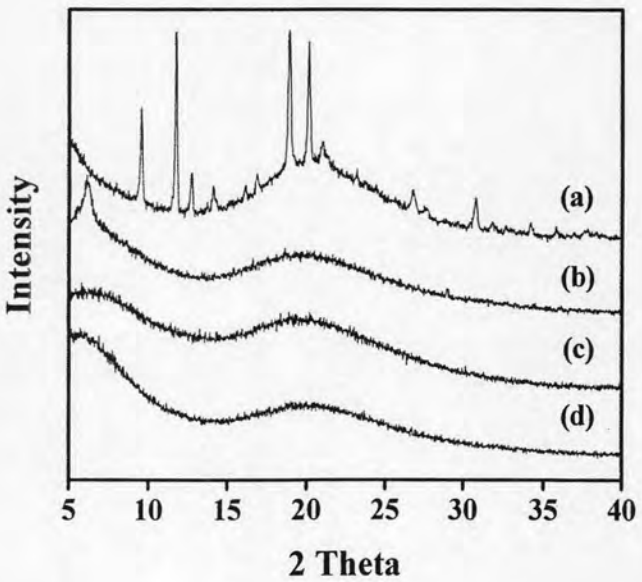

Figure 4.20 XRD patterns of (a) NiSalOMe$_2$trien-MDI-PEG;
(b) ZnSalOMe$_2$trien-MDI-PEG; (c) NiSalOMe$_2$trien-MDI-TEG;
(d) ZnSalOMe$_2$trien-MDI-TEG

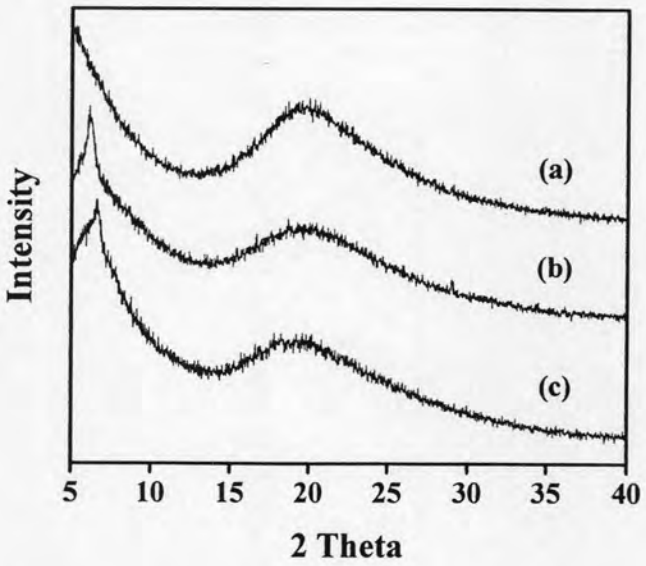

Figure 4.21 XRD patterns of ZnSalOMe$_2$trien-MDI-PEG at the mole ratios of ZnSalOMe$_2$trien:MDI:PEG were (a) 0.5:2:1.5; (b) 1:2:1; (c) 1.5:2:0.5

4.3.1.6 Thermogravimetric analysis and flame retardancy

4.3.1.6.1 MSalOMe$_2$trien-MDI-dialcohols PUUs

The temperature at 5% weight loss (T_5) of metal-containing PUUs (Table 4.11) were in the range 257-293°C, which were lower than those of their corresponding metal-containing polyureas (MSalOMe$_2$trien-MDI). For zinc-containing PUUs based on MDI, their TGA results showed that they had higher char yield at 600°C than ZnSalOMe$_2$trien-MDI. The presence of different dialcohols in the polymer backbone didn't affect their char yields (Figures 4.22-4.23), except for ZnSalOMe$_2$trien-MDI-TEG, which had slightly less char yield than the other MDI-based zinc-containing PUUs. Comparing between nickel-containing PUUs based on MDI and NiSalOMe$_2$trien-MDI, the presence of dialcohols in the polyurethane-urea didn't affect their char yield. MDI-based zinc-containing PUUs showed higher T_5 and char yield than nickel-containing PUUs and they also showed lower decomposition rate than nickel-containing PUUs and reference polyurethane. In comparison to poly(urethane-imide) [10], poly(urethane-imide-imide) [11] and phosphorus-containing polyurethane [42], the obtained polymers exhibited higher char yield at 600°C.

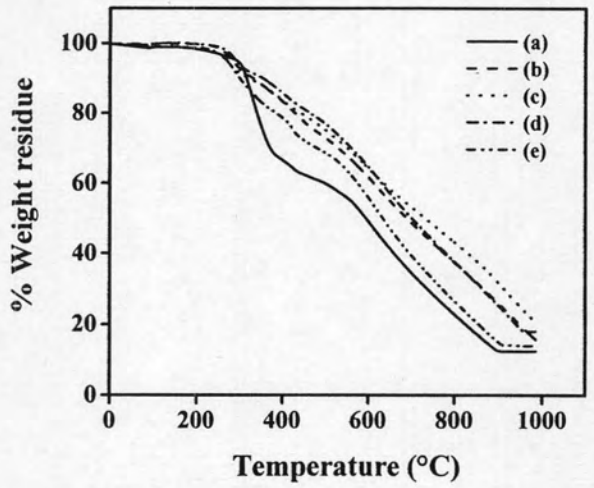

Figure 4.22 TGA thermograms of (a) ZnSalOMe$_2$trien-MDI; (b) ZnSalOMe$_2$trien-MDI-BPA; (c) ZnSalOMe$_2$trien-MDI-HMDO; (d) ZnSalOMe$_2$trien-MDI-PEG; (e) ZnSalOMe$_2$trien-MDI-TEG

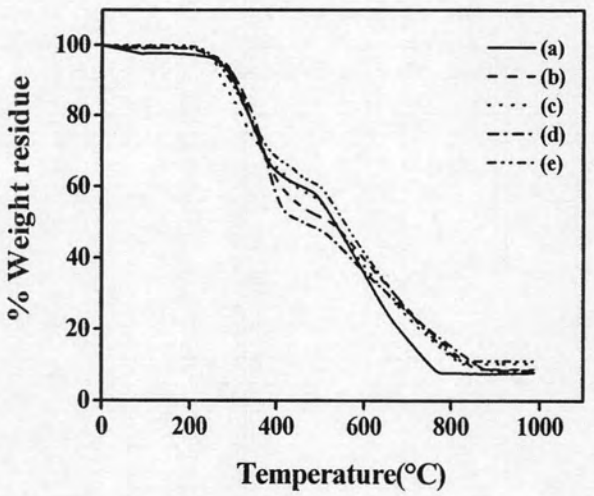

Figure 4.23 TGA thermograms of (a) NiSalOMe$_2$trien-MDI; (b) NiSalOMe$_2$trien-MDI-BPA; (c) NiSalOMe$_2$trien-MDI-HMDO; (d) NiSalOMe$_2$trien-MDI-PEG; (e) NiSalOMe$_2$trien-MDI-TEG

Table 4.11 TGA data of MDI-based metal-containing polyureas, polyurethane-ureas and reference polyurethanes

Polymer	T_5 (°C)	Weight loss (%) at different temperature (°C)			LOI
		300	600	800	
ZnSalOMe$_2$trien-MDI	295	6	51	77	27
NiSalOMe$_2$trien-MDI	268	10	64	92	31
ZnSalOMe$_2$trien-MDI-HMDO	270	9	36	57	35
NiSalOMe$_2$trien-MDI-HMDO	258	15	62	87	23
MDI-HMDO	279	19	82	97	19
ZnSalOMe$_2$trien-MDI-BPA	284	7	38	63	32
NiSalOMe$_2$trien-MDI-BPA	279	8	60	86	23
MDI-BPA	262	15	72	94	20
ZnSalOMe$_2$trien-MDI-TEG	271	10	44	73	28
NiSalOMe$_2$trien-MDI-TEG	264	12	58	87	23
MDI-TEG	227	25	78	97	19
ZnSalOMe$_2$trien-MDI-PEG	293	6	35	62	33
NiSalOMe$_2$trien-MDI-PEG	273	8	64	85	24
MDI-PEG	249	18	74	95	20

4.3.1.6.2 MSalOMe$_2$trien-HMDI-dialcohols PUUs

T_5 of HMDI-based metal-containing PUUs (Table 4.12) were in the range 253-280°C which were lower than their corresponding polyureas (MSalOMe$_2$trien-HMDI). Char yields at 600°C of zinc- and nickel-containing PUUs based on HMDI weren't affected by different dialcohols in the polymer chain. They were in the range 26-37% of starting weight. Comparing to MSalOMe$_2$trien-HMDI, the presence of dialcohols in metal-containing PUUs did not affect their char yields (Figures 4.24 and 4.25). HMDI-based zinc-containing PUUs showed lower T_5 but higher char yields than their corresponding nickel-containing PUUs. HMDI-based metal-containing PUUs exhibited lower char yields than MDI-based metal-containing PUUs because of the present of aromatic ring in MDI. Most metal-containing PUUs showed lower decomposition rate but higher char yield than reference polyurethanes synthesized without metal complexes.

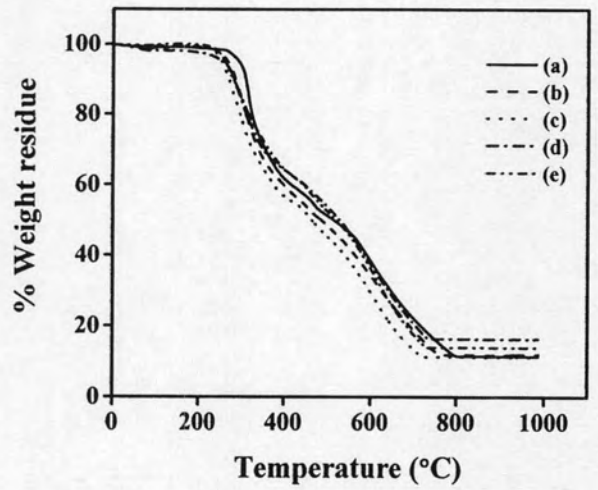

Figure 4.24 TGA thermograms of (a) ZnSalOMe$_2$trien-HMDI; (b) ZnSalOMe$_2$trien-HMDI-BPA; (c) ZnSalOMe$_2$trien-HMDI-HMDO; (d) ZnSalOMe$_2$trien-HMDI-PEG; (e) ZnSalOMe$_2$trien-HMDI-TEG

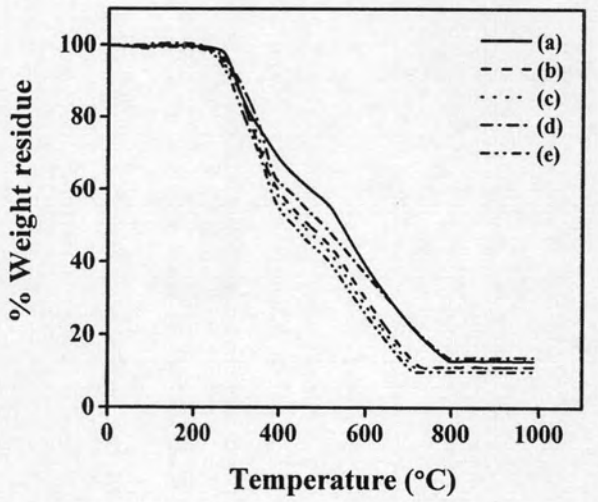

Figure 4.25 TGA thermograms of (a) NiSalOMe$_2$trien-HMDI; (b) NiSalOMe$_2$trien-HMDI-BPA; (c) NiSalOMe$_2$trien-HMDI-HMDO; (d) NiSalOMe$_2$trien-HMDI-PEG; (e) NiSalOMe$_2$trien-HMDI-TEG

Table 4.12 TGA data of HMDI-based metal-containing polyureas, polyurethane-ureas and reference polyurethanes

Polymer	T_5 (°C)	Weight loss (%) at different temperature (°C)			LOI
		300	600	800	
ZnSalOMe$_2$trien-HMDI	294	6	62	89	22
NiSalOMe$_2$trien-HMDI	283	11	61	87	23
ZnSalOMe$_2$trien-HMDI-HMDO	253	21	71	89	22
NiSalOMe$_2$trien-HMDI-HMDO	269	11	72	89	22
HMDI-HMDO	319	2	94	97	18
ZnSalOMe$_2$trien-HMDI-BPA	268	16	66	88	22
NiSalOMe$_2$trien-HMDI-BPA	273	11	70	89	22
HMDI-BPA	282	9	92	99	18
ZnSalOMe$_2$trien-HMDI-TEG	261	15	64	86	23
NiSalOMe$_2$trien-HMDI-TEG	262	15	74	90	22
HMDI-TEG	238	22	92	93	18
ZnSalOMe$_2$trien-HMDI-PEG	257	16	63	84	24
NiSalOMe$_2$trien-HMDI-PEG	280	9	63	86	23
HMDI-PEG	246	17	90	93	18

Flame retardant properties of metal-containing PUUs were compared from their limiting oxygen index (LOI) values (Tables 4.11 and 4.12). LOI is the minimum concentration of oxygen, expressed as volume present, in a mixture of oxygen and nitrogen that will support flaming combustion of a material. A polymer having an LOI greater than 21 does not burn in atmosphere since the oxygen content in atmosphere is 21%. The polymer with higher LOI is more flame retardant. LOI was calculated from char yield by Van Krevelen and Hoftyzer equation [39-41].

Van Krevelen and Hoftyzer equation: LOI = 17.5 + 0.4CR

Where CR = char yield at 800°C

All metal-containing PUUs showed the same LOI value in the range 22-24 which are comparable to phosphorus-containing polyurethanes [42]. The metal-containing PUUs based on MDI showed slightly higher flame retardancy than those

derived from HMDI because of the presence of aromatic rings in the main chain of polymers.

4.4 Synthesis of metal-containing copolyureas (MSalOMe$_2$trien-coPUs)

4.4.1 Synthesis of metal-containing copolyureas (MSalOMe$_2$trien-coPUs) from the reaction between MSalOMe$_2$trien, diisocyanates and diamines

The purpose of this work was to add urea linkages into the polymer structure by addition of diamines during the polymerization. It was expected that these copolyureas would show good thermal stability because of additional hydrogen bonding between donor N-H groups and acceptor urea carbonyl groups (Figure 4.26). Synthesis of copolyureas containing MSalOMe$_2$trien complexes were done by polyaddition reaction between MSalOMe$_2$trien, diisocyanates and diamines as shown in Scheme 4.7. The diisocyanates used were HMDI and MDI to obtain the polymer containing aliphatic and aromatic part, respectively. Different diamines having aromatic, aliphatic and aliphatic containing ether group were used to study effects on the polymer properties. The blank polyureas without metal complexes were also prepared by the reaction of diisocyanates and diamines to study the influence of metal complexes on the thermal property of polymers.

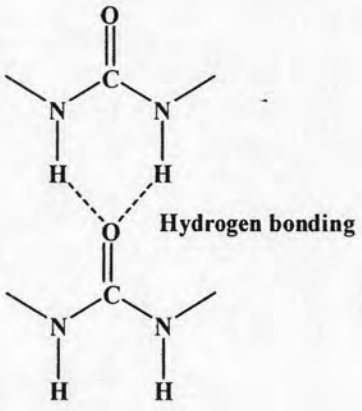

Figure 4.26 Hydrogen bonding of polyurea

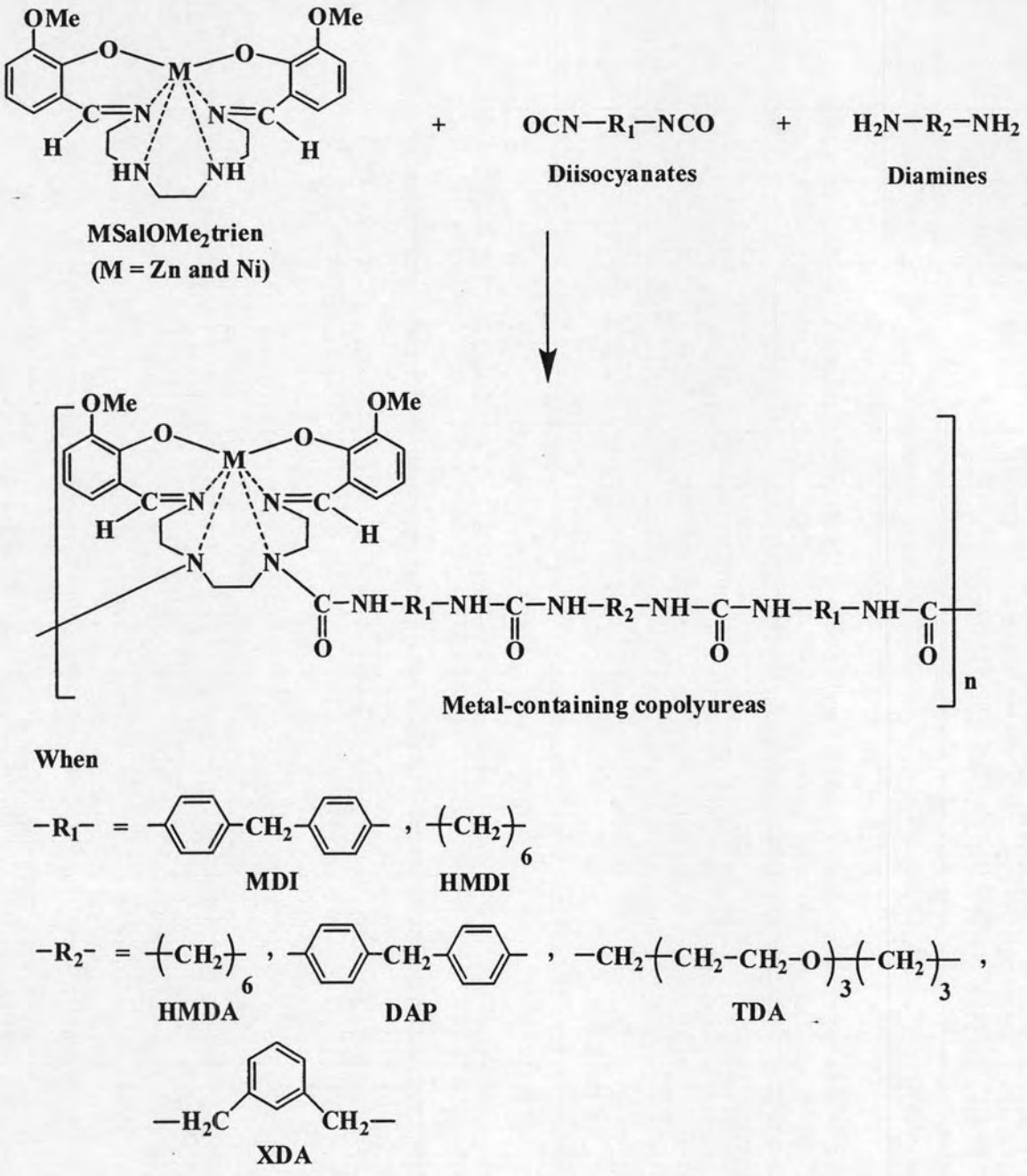

Scheme 4.7 Synthesis of MSalOMe$_2$trien-coPUs from the reaction between MSalOMe$_2$trien, diisocyanates and diamines

All metal-containing copolyureas were synthesized by taking the mole ratio of MSalOMe$_2$trien:diisocyanate:diamine as 1:2:1. The yield of copolyureas and reference polyureas were found to be in the range 78-96% and 53-96%, respectively (Table 4.13).

Table 4.13 Synthesis data of MSalOMe$_2$trien-coPUs and reference polyureas

Polymers	Yield (%)	External appearance
ZnSalOMe$_2$trien-MDI-HMDA	90	Yellowish brown powder
ZnSalOMe$_2$trien-MDI-DAP	85	Orange brown powder
ZnSalOMe$_2$trien-MDI-XDA	88	Orange yellow powder
ZnSalOMe$_2$trien-MDI-TDA	84	Orange yellow powder
NiSalOMe$_2$trien-MDI-HMDA	91	Dark brown powder
NiSalOMe$_2$trien-MDI-DAP	96	Brown powder
NiSalOMe$_2$trien-MDI-XDA	92	Brown powder
NiSalOMe$_2$trien-MDI-TDA	78	Light brown powder
ZnSalOMe$_2$trien-HMDI-HMDA	90	Light brown powder
ZnSalOMe$_2$trien-HMDI-DAP	85	Brown orange powder
ZnSalOMe$_2$trien-HMDI-XDA	88	Brown powder
ZnSalOMe$_2$trien-HMDI-TDA	84	Brown powder
NiSalOMe$_2$trien-HMDI-HMDA	91	Dark brown powder
NiSalOMe$_2$trien-HMDI-DAP	96	Dark brown powder
NiSalOMe$_2$trien-HMDI-XDA	92	Brown powder
NiSalOMe$_2$trien-HMDI-TDA	78	Dark brown powder
MDI-HMDA	71	White powder
MDI-DAP	75	yellow powder
MDI-XDA	66	White powder
MDI-TDA	84	White powder
HMDI-HMDA	64	White powder
HMDI-DAP	53	White powder
HMDI-XDA	74	White powder
HMDI-TDA	96	White powder

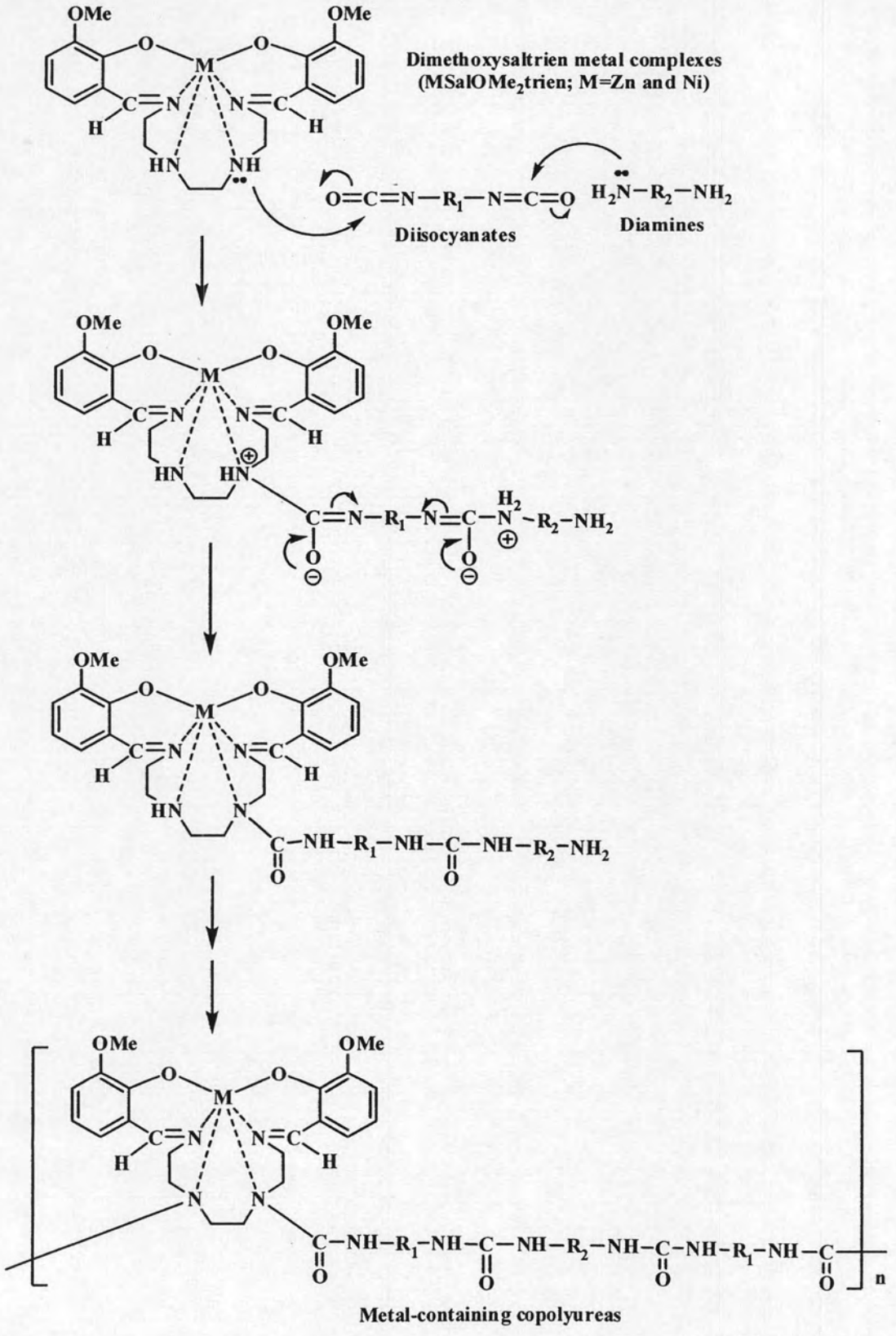

Scheme 4.8 Possible mechanism of the reaction between $MSalOMe_2trien$, diisocyanates and diamines

The possible polymerization mechanism is proposed that the NH of metal complexes and NH_2 of diamines undergo a reaction with isocyanate group to give urea linkages (Schemes 4.8).

4.4.2 Characterization of MSalOMe$_2$trien-containing coPUs

4.4.2.1 IR spectroscopy

IR spectra and data of the MSalOMe$_2$trien-containing coPUs are shown in Figures 4.27 and 4.28 and Tables 4.14-4.15, respectively. All metal-containing coPUs had similar IR absorption band. They showed intense absorption bands between 3417-3313 cm^{-1} that could be attributed to N-H stretching. The absorption bands at 2918-2856 cm^{-1} were due to the asymmetrical and symmetrical C-H stretching of methylene and methyl groups. The band around 1670-1621 cm^{-1} were attributed to the carbonyl stretching of urea group (amide I) overlapped with C=N stretching. All above the absorption bands indicated the typical characteristic of polyurea. The absorption band of urea carbonyl of MDI-based metal-containing copolyureas appeared at higher frequency than the HMDI-based metal-containing copolyureas because of electron-withdrawing group of aromatic ring in MDI. Electron-withdrawing groups attached to the nitrogen increase the frequency of absorption since they effectively complete with the carbonyl oxygen for the electron of nitrogen, thus increasing the force constant of the C=O bond [33].

Figure 4.29 show IR spectra of reference polyureas. The important characteristic absorption bands are as follows: 3308-3352 cm^{-1} (N-H stretching), 2932-2848 cm^{-1} (C-H stretching) and 1654-1629 cm^{-1} (C=O stretching of urea).

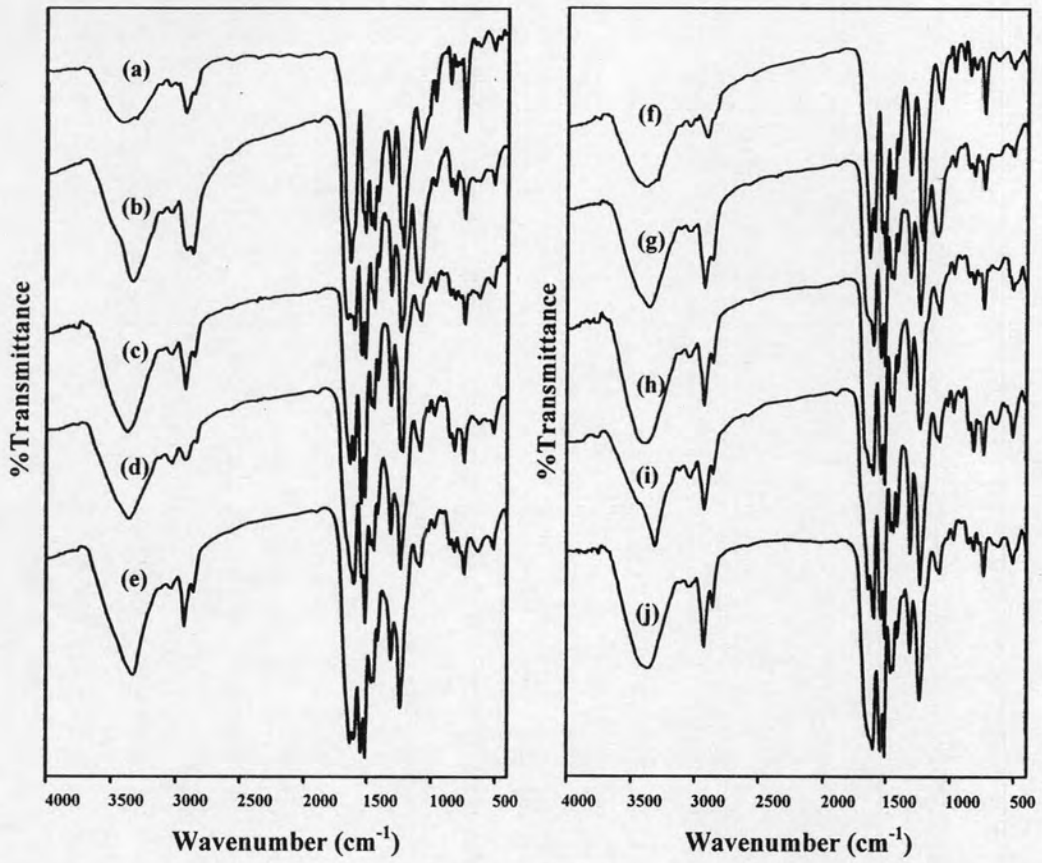

Figure 4.27 IR spectra of MSalOMe$_2$trien-containing coPUs

(a) ZnSalOMe$_2$trien-MDI; (b) ZnSalOMe$_2$trien-MDI-TDA;

(c) ZnSalOMe$_2$trien-MDI-XDA; (d) ZnSalOMe$_2$trien-MDI-DAP;

(e) ZnSalOMe$_2$trien-MDI-HMDA; (f) NiSalOMe$_2$trien-MDI;

(g) NiSalOMe$_2$trien-MDI-TDA; (h) NiSalOMe$_2$trien-MDI-XDA;

(i) NiSalOMe$_2$trien-MDI-DAP; (j) NiSalOMe$_2$trien-MDI-HMDA

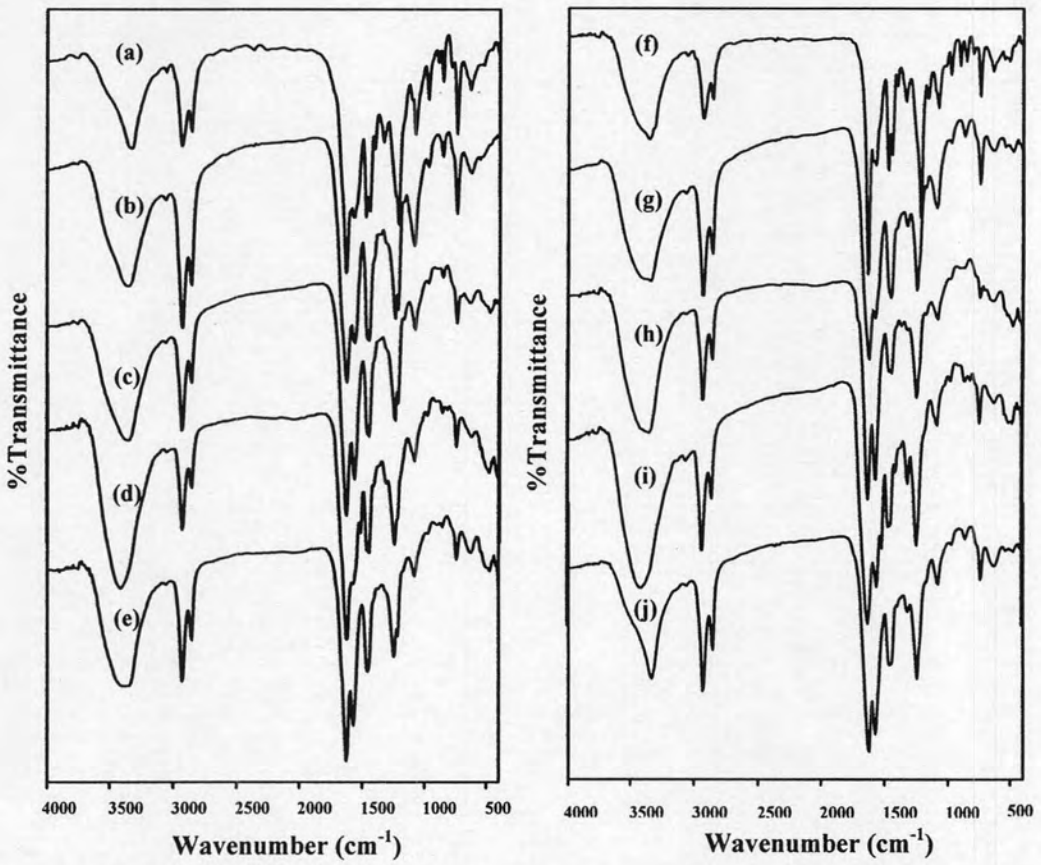

Figure 4.28 IR spectra of $MSalOMe_2trien$-containing coPUs

(a) $ZnSalOMe_2trien$-HMDI; (b) $ZnSalOMe_2trien$-HMDI-TDA;

(c) $ZnSalOMe_2trien$-HMDI-XDA; (d) $ZnSalOMe_2trien$-HMDI-DAP;

(e) $ZnSalOMe_2trien$-HMDI-HMDA; (f) $NiSalOMe_2trien$-HMDI;

(g) $NiSalOMe_2trien$-HMDI-TDA; (h) $NiSalOMe_2trien$-HMDI-XDA;

(i) $NiSalOMe_2trien$-HMDI-DAP; (j) $NiSalOMe_2trien$-HMDI-HMDA

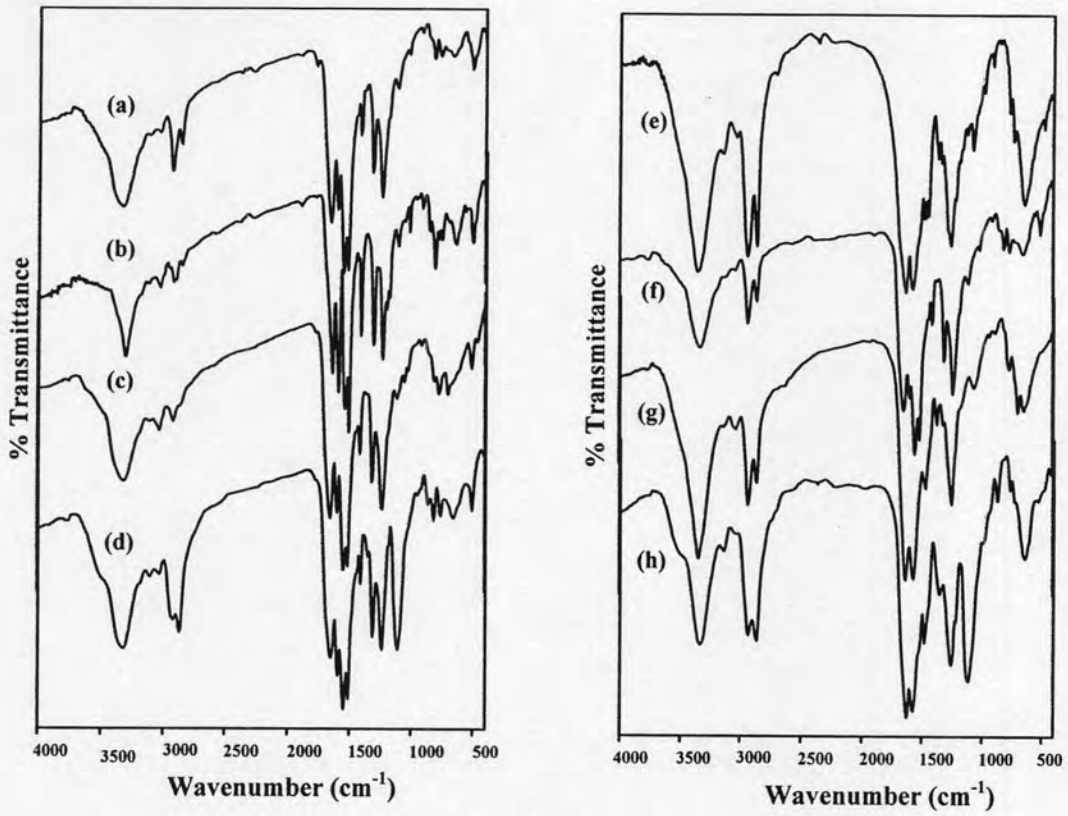

Figure 4.29 IR spectra of reference polyureas

(a) MDI-HMDA; (b) MDI-DAP; (c) MDI-XDA; (d) MDI-TDA; (e) HMDI-HMDA; (f) HMDI-DAP; (g) HMDI-XDA; (h) HMDI-TDA

Table 4.14 Metal-containing PUs based on MDI

Absorption band (cm^{-1}) [33]	Absorption band (cm^{-1}) [34]	Absorption band (cm^{-1})	Assignment [a]
3330-3060	3750-3050	3382-3313	N-H stretching vibration
2900-2800	3000-2800	2928-2856	CH_2 symmetric and antisymmetric stretching vibration
1640	1800-1600	1670-1634	C=N and C=O of urea group stretching vibration (amide I)
1800-1600, 1500-1400	-	1605-1600, 1518-1512	Aromatic ring stretching vibration
1570-1515	1589-1500	1548-1544	N-H bending (amide II) and C-N stretching vibration
-	1461-1453	1465-1444	CH_2 scissoring and CH_2 bending
-	1292-1200	1239-1221	In plane N-H and C-N stretching vibration (amide III)
-	1070	1104-1082	C-N stretching vibration
900-800, 700-650	-	741-740	C-H out-of-plane deformation of 1,2,3-trisubstituted benzene

Table 4.15 Metal-containing PUs based on HMDI

Absorption band (cm^{-1}) [33]	Absorption band (cm^{-1}) [34]	Absorption band (cm^{-1})	Assignment [a]
3330-3060	3750-3050	3417-3333	N-H stretching vibration
2900-2800	3000-2800	2928-2856	CH_2 symmetric and antisymmetric stretching vibration
1640	1800-1600	1628-1621	C=N and C=O of urea group stretching vibration (amide I)
1570-1515	1589-1500	1574-1551	N-H bending (amide II) and C-N stretching vibration
1800-1600, 1500-1400	-	1515	Aromatic ring stretching vibration
-	1461-1453	1463-1445	CH_2 scissoring and CH_2 bending
-	1292-1200	1248-1218	In plane N-H and C-N stretching vibration (amide III)
-	1070	1089-1082	C-N stretching vibration
900-800, 700-650	-	740-738	C-H out-of-plane deformation of 1,2,3-trisubstituted benzene

[a] The amide I mode is primary a C=O stretching band. The amide II mode is an out-of-phase combination of largely N-H in plane bending and C-N stretching. Amide III mode is the in-phase combination of N-H in-plane bending and C-N stretching.

IR spectra of $MSalOMe_2trien$, $MSalOMe_2trien$-containing polyureas, $MSalOMe_2trien$-containing copolyureas and reference polyureas were compared as shown in Figures 4.30 and 4.31. It could be seen that urea carbonyl absorption was not clearly observed because it overlapped with imine peaks.

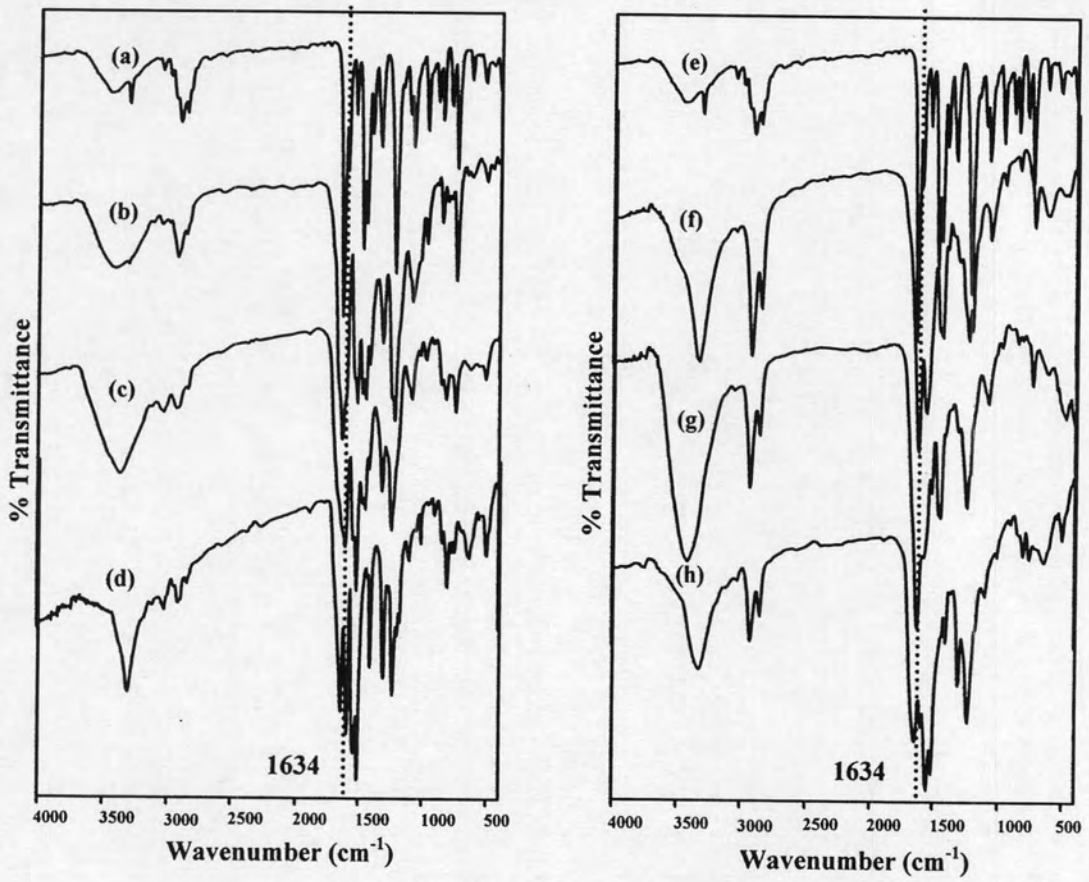

Figure 4.30 IR spectra of (a) $ZnSalOMe_2trien$; (b) $ZnSalOMe_2trien$-MDI; (c) $ZnSalOMe_2trien$-MDI-DAP; (d) MDI-DAP; (e) $ZnSalOMe_2trien$; (f) $ZnSalOMe_2trien$-HMDI; (g) $ZnSalOMe_2trien$-HMDI-DAP; (h) HMDI-DAP

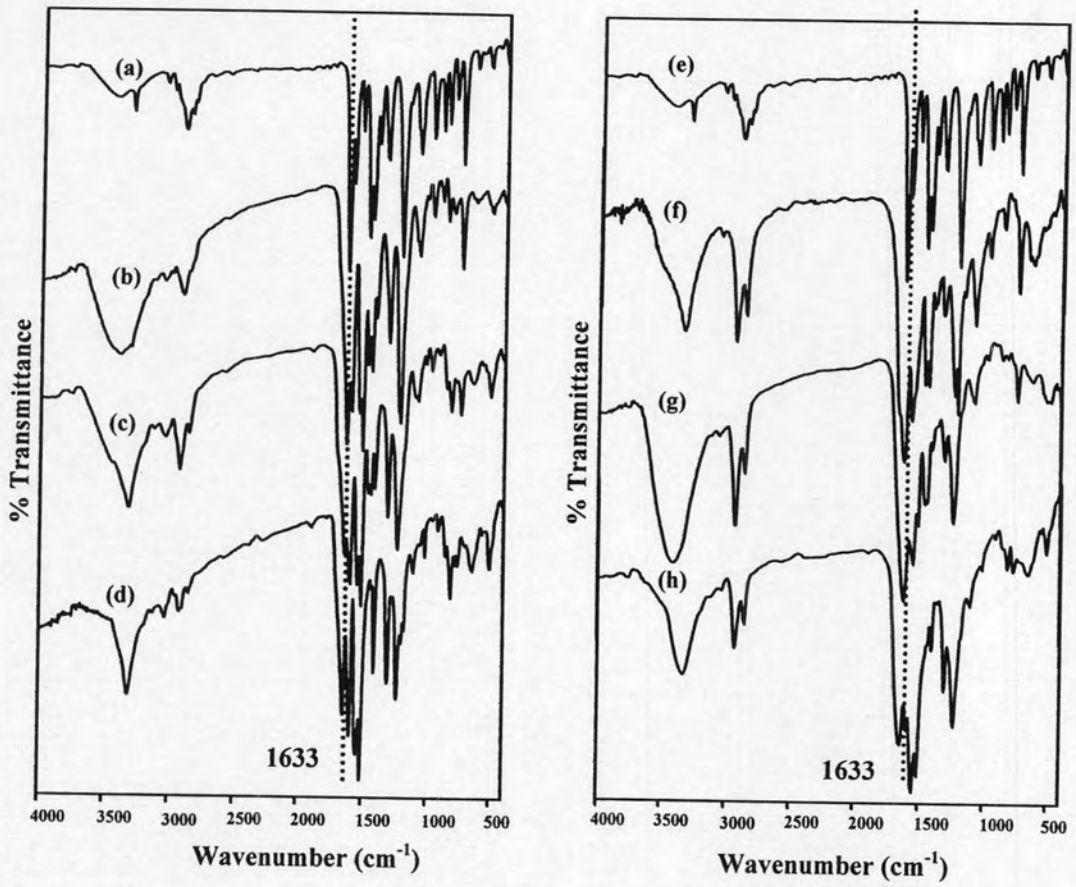

Figure 4.31 IR spectra of (a) $NiSalOMe_2trien$; (b) $NiSalOMe_2trien$-MDI; (c) $NiSalOMe_2trien$-MDI-DAP; (d) MDI-DAP; (e) $NiSalOMe_2trien$; (f) $NiSalOMe_2trien$-HMDI; (g) $NiSalOMe_2trien$-HMDI-DAP; (h) HMDI-DAP

4.4.2.2 ^{1}H NMR spectroscopy

^{1}H NMR spectra and data of MSalOMe$_2$trien-containing copolyurea are shown in Figures 4.32-4.39 and Table 4.16, respectively. All of them showed the important characteristic peaks as follows: CH=N protons appeared at 8.97-7.84 ppm as multiplet peaks. The absorption of aromatic protons appeared in the range 7.61-5.99 ppm. N-H protons of urea group were observed at 8.97-8.38, 6.51-5.60, and 4.98-4.68 ppm as broad peaks. The protons of methoxy, methylene attached to aromatic, and methylene group appeared in the range 4.09-0.70 ppm. Comparing between HMDI- and MDI-based metal-containing copolyureas, aromatic proton of MSalOMe$_2$trien in MDI-based polymers appeared as broad peaks so they overlapped with aromatic protons of MDI. The aromatic protons of MSalOMe$_2$trien could be observed only in ZnSalOMe$_2$trien-MDI-XDA at 6.67 and 6.10 ppm.

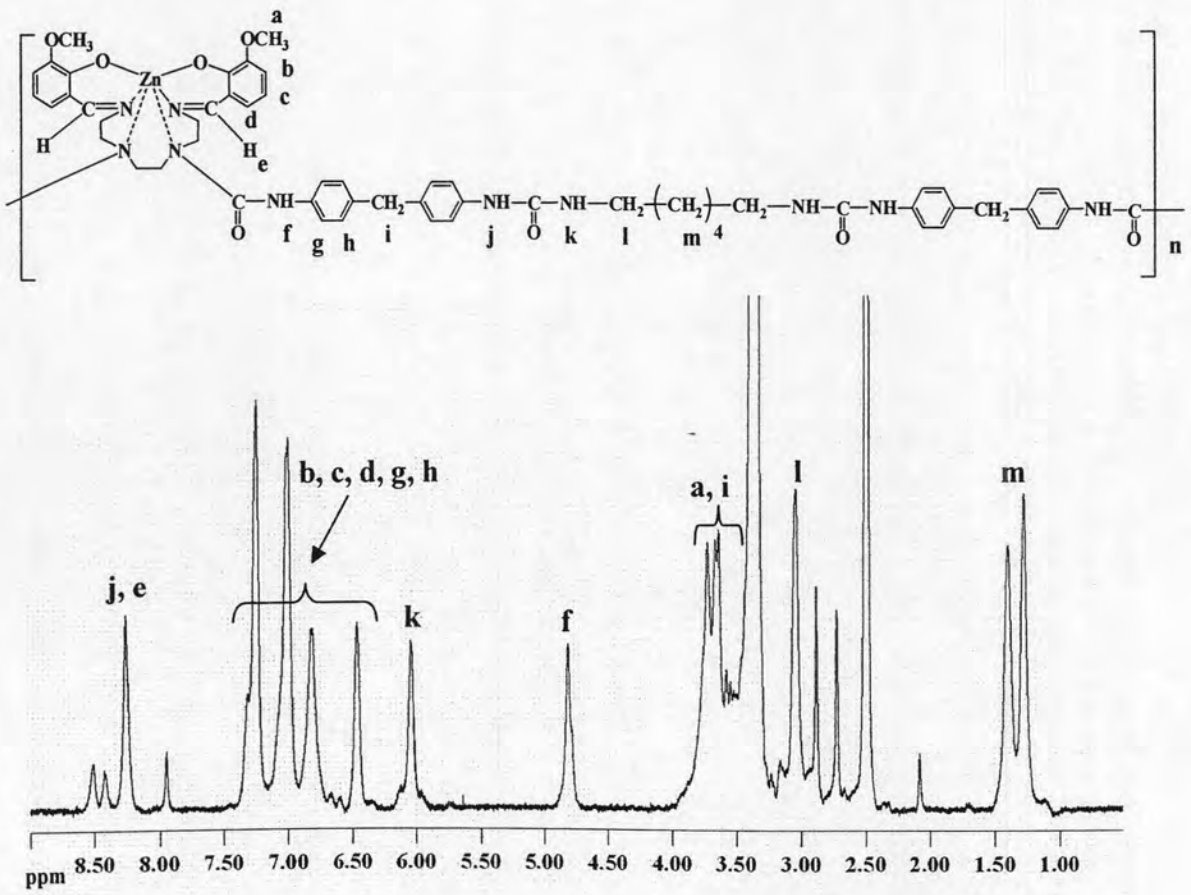

Figure 4.32 ^{1}H NMR spectrum of ZnSalOMe$_2$trien-MDI-HMDA in DMSO-d_6

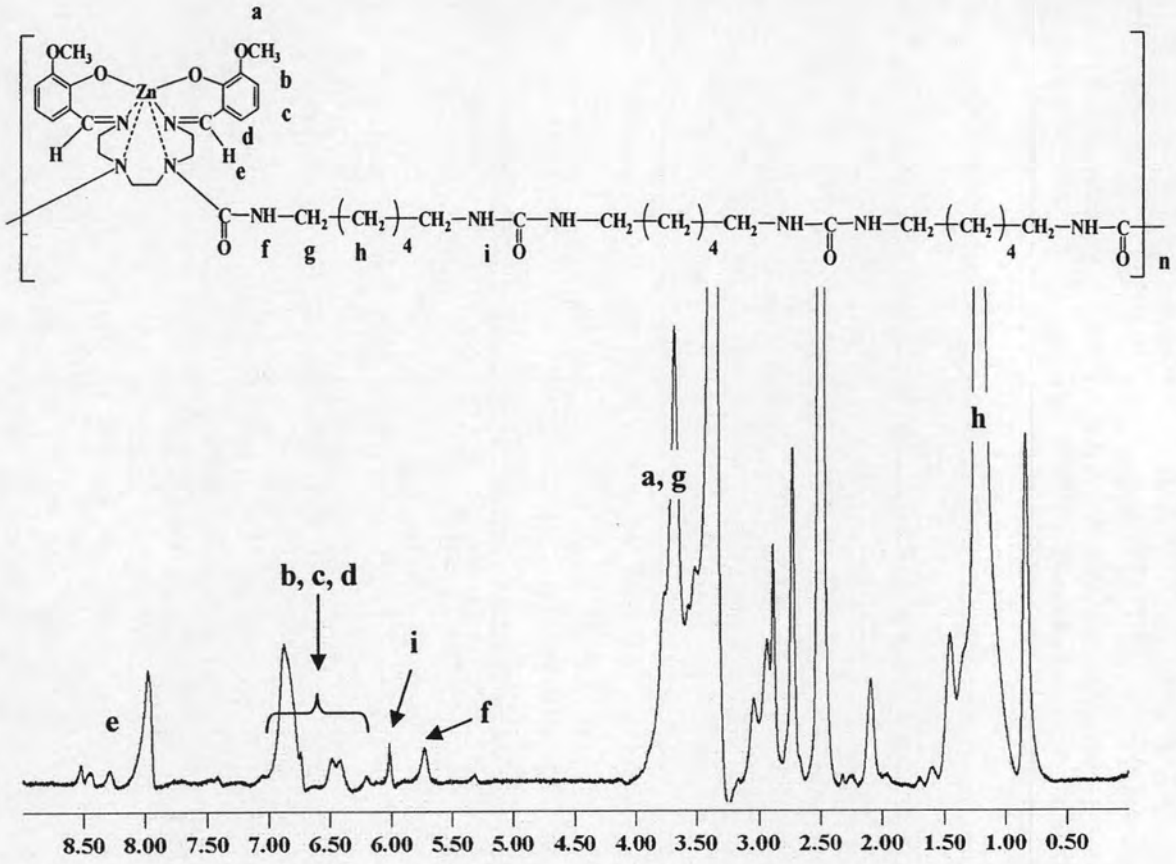

Figure 4.33 ^{1}H NMR spectrum of ZnSalOMe$_2$trien-HMDI-HMDA in DMSO-d_6

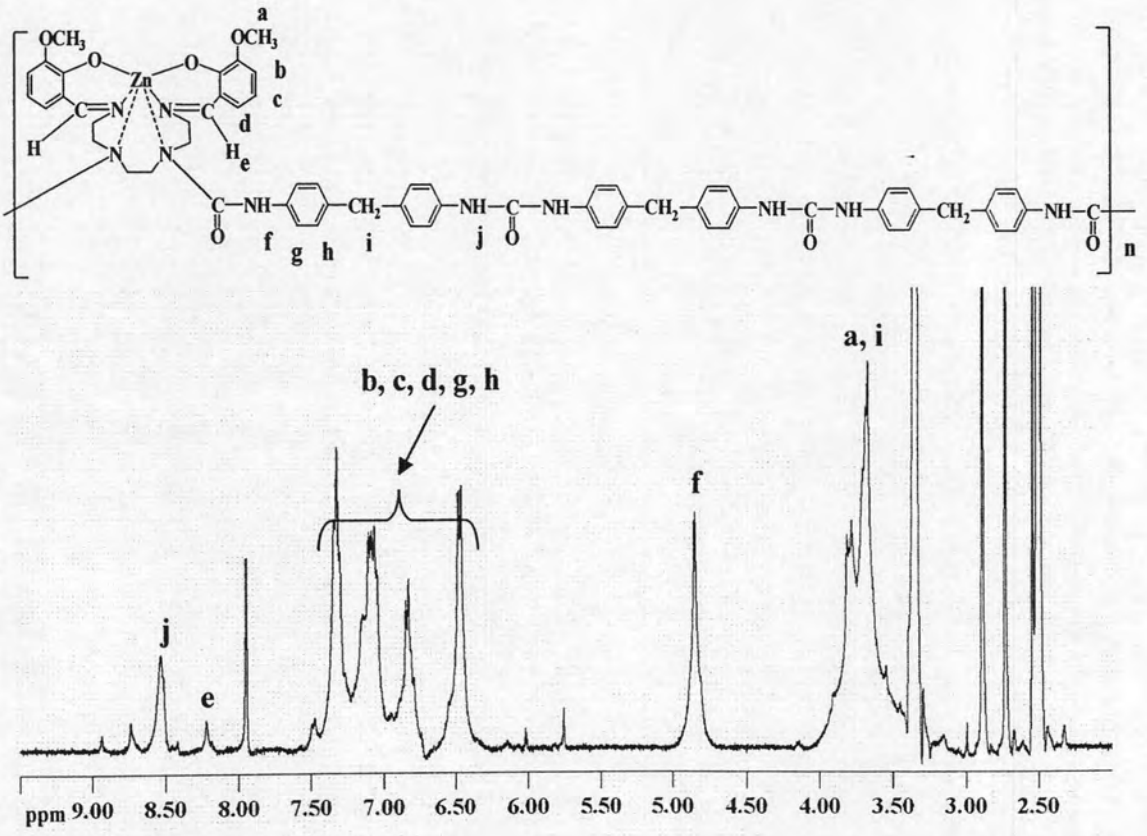

Figure 4.34 ^{1}H NMR spectrum of ZnSalOMe$_2$trien-MDI-DAP in DMSO-d_6

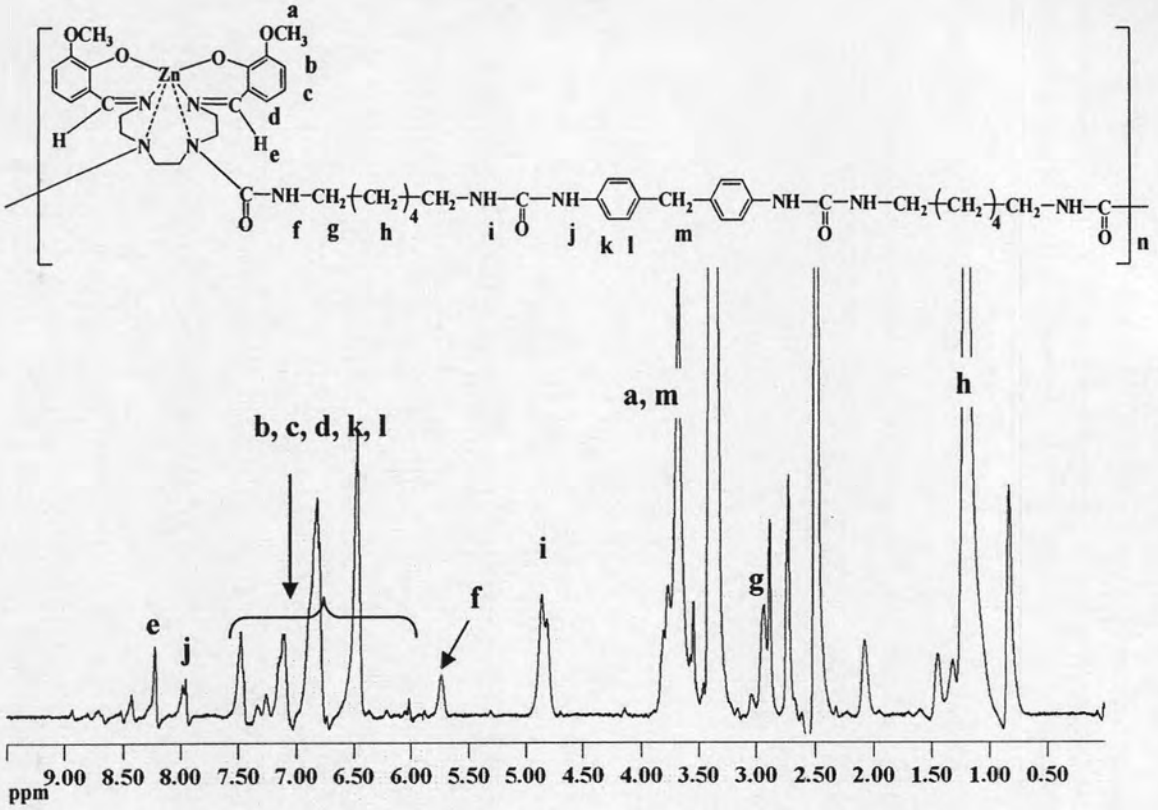

Figure 4.35 ^{1}H NMR spectrum of ZnSalOMe$_2$trien-HMDI-DAP in DMSO-d_6

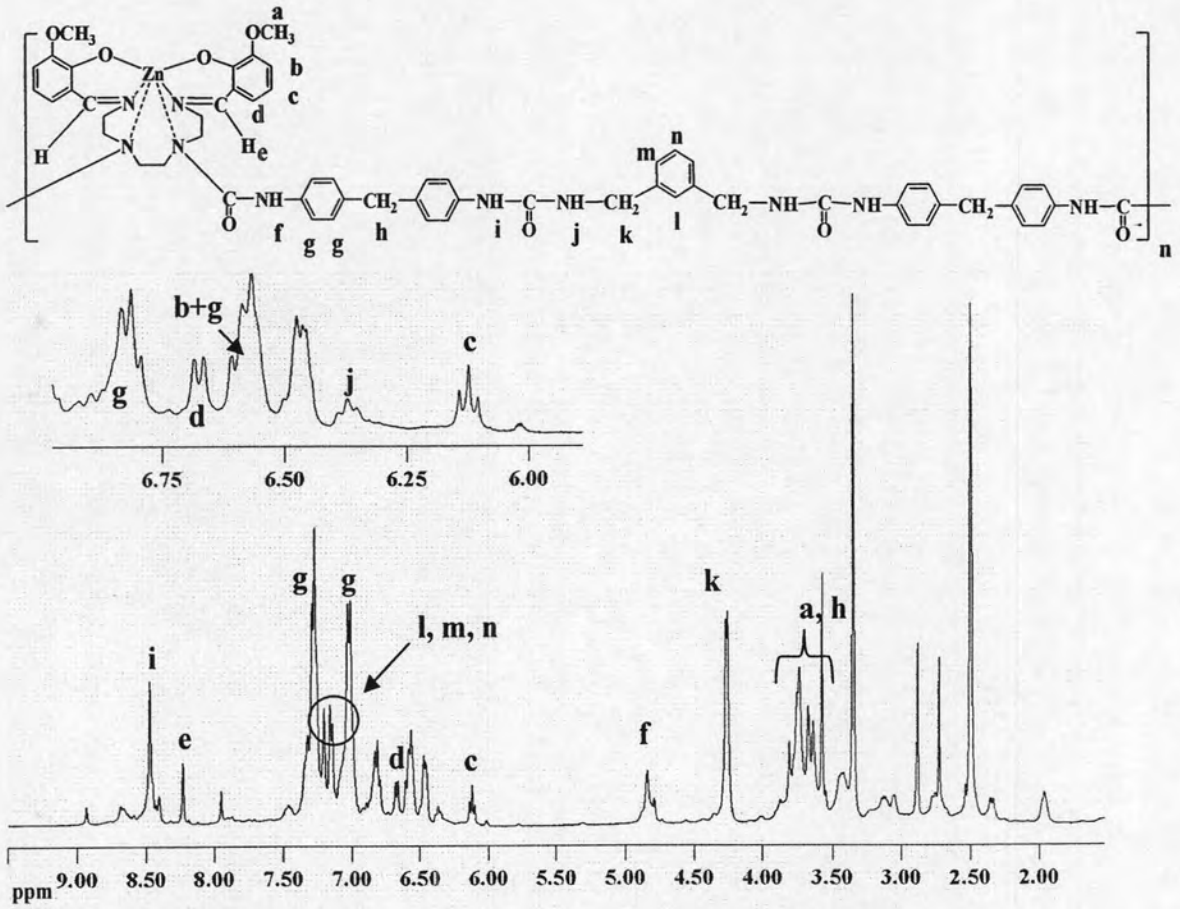

Figure 4.36 ^{1}H NMR spectrum of ZnSalOMe$_2$trien-MDI-XDA in DMSO-d_6

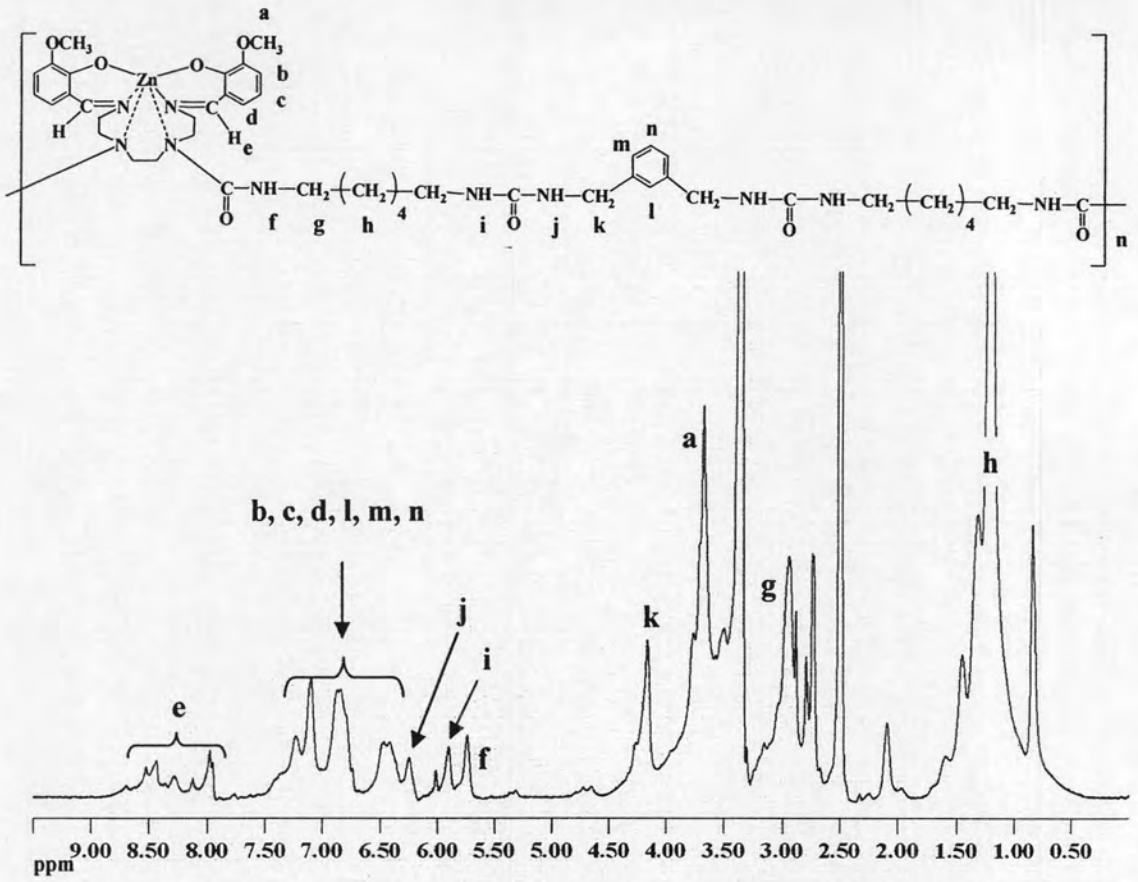

Figure 4.37 ^{1}H NMR spectrum of ZnSalOMe$_2$trien-HMDI-XDA in DMSO-d_6

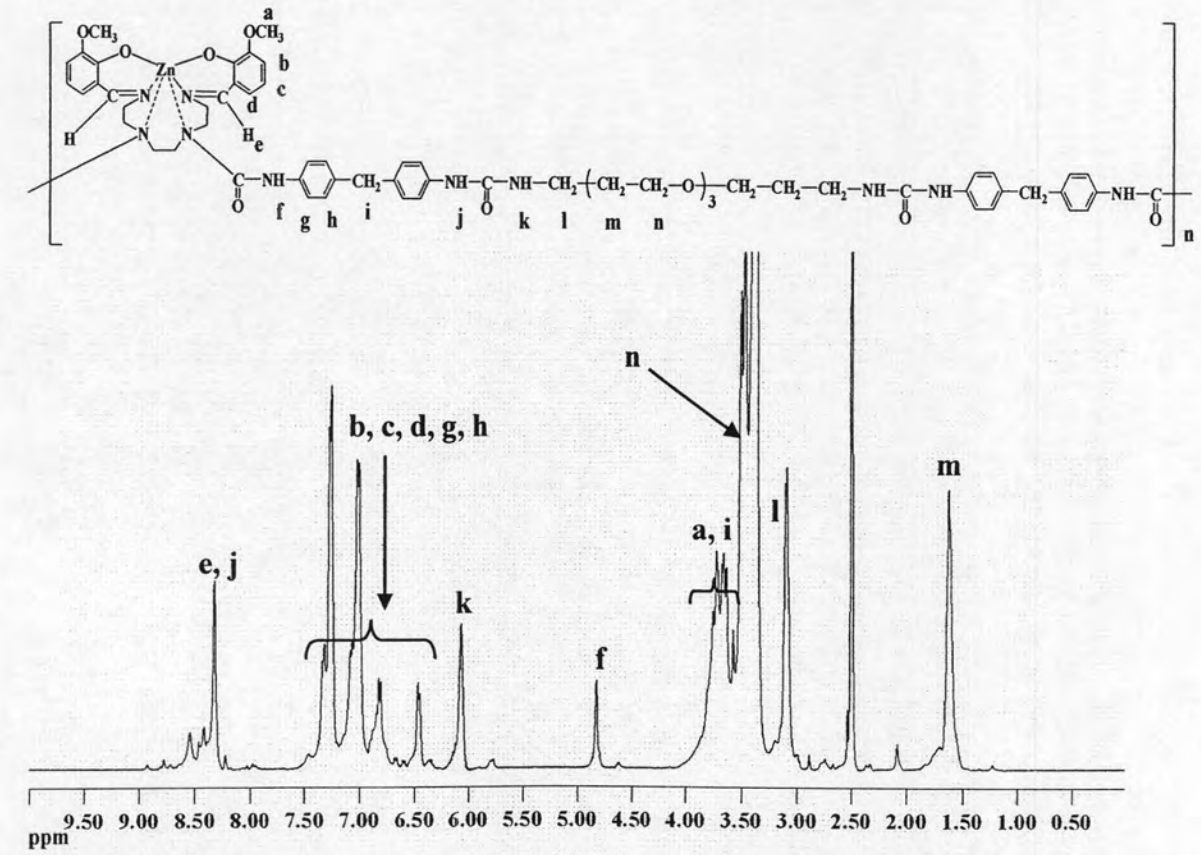

Figure 4.38 ^{1}H NMR spectrum of ZnSalOMe$_2$trien-MDI-TDA in DMSO-d_6

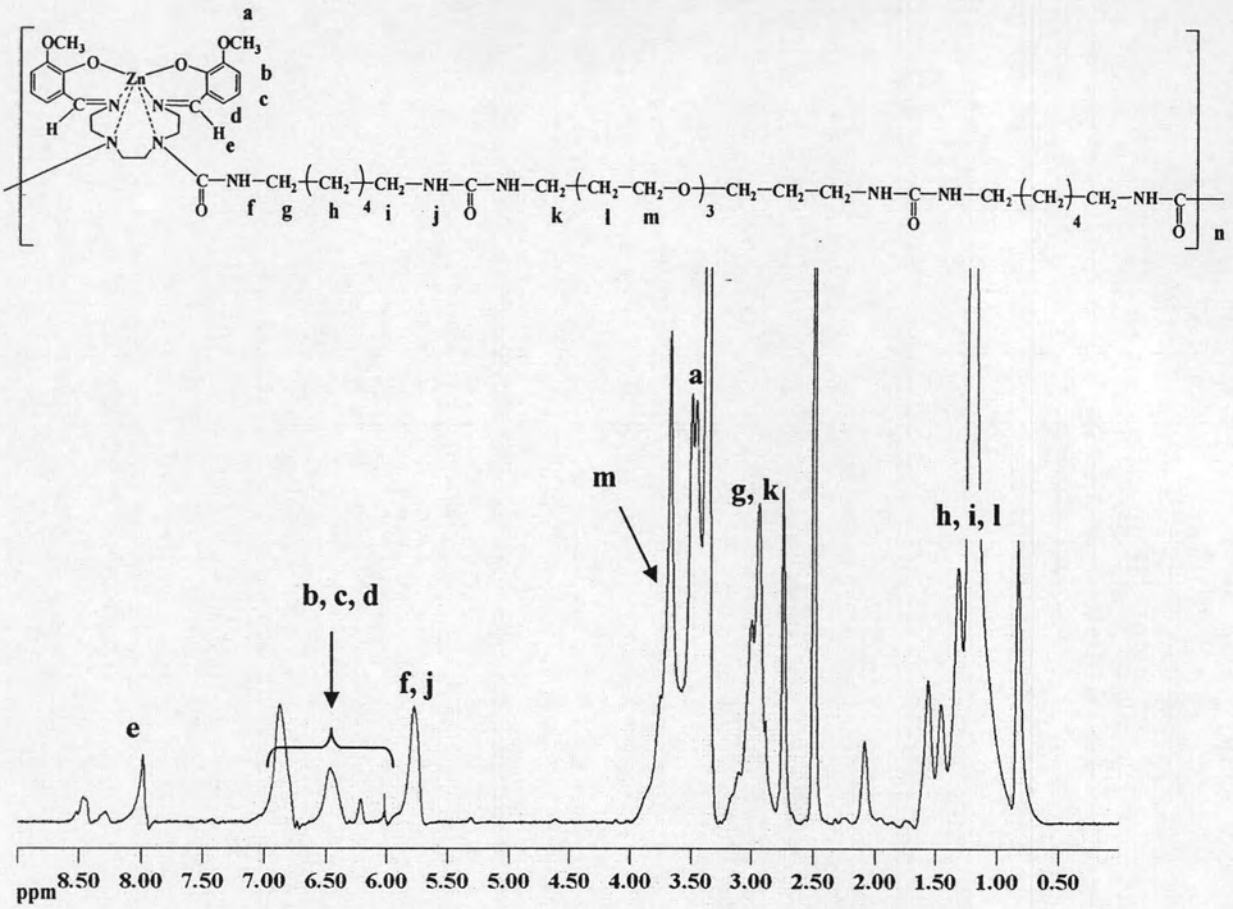

Figure 4.39 ^{1}H NMR spectrum of ZnSalOMe$_2$trien-HMDI-TDA in DMSO-d_6

Table 4.16 ^{1}H NMR assignment of MSalOMe$_2$trien-containing coPUs

Copolyureas	^{1}H NMR assignment
MDI-based copolyureas	
ZnSalOMe$_2$trien-MDI-HMDA	8.59-8.19 (*brs*, HNC=ON**H**Ar and C**H**=N), 7.33-7.17 (*m*, Ar-**H**), 7.09-6.92 (*m*, Ar-**H**), 6.89-6.75 (*m*, Ar-**H**), 6.54-6.39 (*m*, Ar-**H**), 6.11-5.97 (*brs*, HNC=ON**H**CH$_2$), 4.93-4.68 (*brs*, NC=ON**H**), 3.79-3.54 (*m*, Ar-C**H**$_2$-Ar and OC**H**$_3$), 3.13-2.97 (*m*, HN-C**H**$_2$), 1.52-1.16 (*m*, C**H**$_2$).
ZnSalOMe$_2$trien-MDI-DAP	8.59-8.46 (*m*, HNC=ON**H**Ar), 7.41-7.24 (*m*, Ar-**H**), 7.21-6.99 (*m*, Ar-**H**), 6.90-6.77 (*m*, Ar-**H**), 6.54-6.39 (*m*, Ar-**H**), 4.98-4.72 (*brs*, NC=ON**H**), 4.09-3.40 (*m*, Ar-C**H**$_2$-Ar and OC**H**$_3$).
ZnSalOMe$_2$trien-MDI-XDA	8.57-8.35 (*brs*, HNC=ON**H**Ar), 8.29-8.14 (*m*, C**H**=N), 7.41-7.23 (*m*, Ar-**H**), 7.23-7.11 (*m*, Ar-**H**), 7.11-6.93 (*m*, Ar-**H**), 6.93-6.72 (*m*, Ar-**H**), 6.67 (*d*, J = 7.6 Hz, Ar-**H**), 6.63-6.52 (*m*, Ar-**H**), 6.51-6.42 (*m*, HNC=ON**H**CH$_2$), 6.10 (*t*, J = 7.6 Hz, Ar-**H**), 4.93-4.73 (*m*, NC=ON**H**), 4.33-4.19 (*m*, Ar-C**H**$_2$-NH), 3.94-3.50 (*m*, Ar-C**H**$_2$-Ar and OC**H**$_3$).
ZnSalOMe$_2$trien-MDI-TDA	8.83-7.99(*brs*, C**H**=N and NC=ON**H**Ar), 7.39-7.18 (*m*, Ar-**H**), 7.17-6.92 (*m*, Ar-**H**) 6.92-6.72 (*m*, Ar-**H**), 6.57-6.36 (*m*, Ar-**H**), 6.17-5.99 (*brs*, HNC=ON**H**CH$_2$), 4.90-4.75 (*brs*, NC=ON**H**), 3.85-3.56 (*m*, Ar-C**H**$_2$-Ar and OC**H**$_2$), 3.55-3.44 (*m*, OC**H**$_3$), 3.20-2.95 (*m*, HN-C**H**$_2$), 1.72-1.49 (*m*, C**H**$_2$).

Table 4.16 NMR assignment of MSalOMe$_2$trien-containing coPUs (continued)

Copolyureas	^{1}H NMR assignment
HMDI-based copolyureas	
ZnSalOMe$_2$trien-HMDI-HMDA	8.62-7.84 (*brs*, C**H**=N), 7.15-6.15 (*m*, Ar-**H**), 6.10-5.95 (*brs*, HNC=ON**H**CH$_2$), 5.80-5.67 (*brs*, NC=ON**H**), 3.84-3.58 (*m*, OC**H**$_3$ and HN-C**H**$_2$), 1.51-0.70 (C**H**$_2$).
ZnSalOMe$_2$trien-HMDI-DAP	8.97-8.38 (*brs*, HNC=ON**H**Ar), 8.26-8.19 (*m*, C**H**=N), 7.61-6.37 (*m*, Ar-**H**), 5.98-5.60 (*brs*, NC=ON**H**), 4.93-4.74 (*m*, HNC=ON**H**CH$_2$), 3.88-3.49 (*m*, OC**H**$_3$ and Ar-C**H**$_2$-Ar), 3.02-2.82 (*m*, HN-C**H**$_2$), 1.40-0.90 (*m*, C**H**$_2$).
ZnSalOMe$_2$trien-HMDI-XDA	8.86-7.89 (*m*, C**H**=N), 7.54-6.15 (*m*, Ar-**H** and HNC=ON**H**CH$_2$), 5.99-5.85 (*brs*, HNC=ON**H**CH$_2$Ar), 5.81-5.68 (*brs*, NC=ON**H**), 4.37-4.01 (*m*, Ar-C**H**$_2$), 3.85-3.54 (*m*, OC**H**$_3$), 3.09-2.84 (*m*, HN-C**H**$_2$), 1.60-0.70 (*m*, C**H**$_2$).
ZnSalOMe$_2$trien-HMDI-TDA	8.62-7.85 (*m*, C**H**=N), 7.14-5.99 (*m*, Ar-**H**), 5.88-5.67 (*brs*, NC=ON**H**Ar and NC=ON**H**CH$_2$), 3.67 (*brs*, OC**H**$_3$), 3.50-3.46 (*m*, OC**H**$_2$), 3.09-2.83 (*m*, HN-C**H**$_2$), 1.57-0.70 (*m*, C**H**$_2$).

4.4.2.3 Solubility

The solubility of metal-containing coPUs was tested in various polar and nonpolar solvents (Tables 4.17 and 4.18). Solubility test showed that these metal-containing polymers were insoluble in hexane, toluene, CH_3CN, H_2O, CH_2Cl_2, $CHCl_3$, MeOH and THF. They were soluble in polar solvents such as DMF and DMSO. Metal-containing coPUs showed considerable better solubility than their corresponding metal-containing polyureas and reference polyureas synthesized without metal complexes.

Table 4.17 The solubility of MDI-based metal-containing copolyureas and reference polyureas

Polymers	DMF	Maximum solubility (mg)/ DMSO 1 mL
ZnSalOMe$_2$trien-MDI	-	5
NiSalOMe$_2$trien-MDI	-	5
ZnSalOMe$_2$trien-MDI-HMDA	-	-
ZnSalOMe$_2$trien-MDI-DAP	±	143
ZnSalOMe$_2$trien-MDI-XDA	++	580
ZnSalOMe$_2$trien-MDI-TDA	++	767
NiSalOMe$_2$trien-MDI-HMDA	-	-
NiSalOMe$_2$trien-MDI-DAP	++	489
NiSalOMe$_2$trien-MDI-XDA	++	687
NiSalOMe$_2$trien-MDI-TDA	++	829
MDI-HMDA	-	5
MDI-DAP	-	5
MDI-XDA	+	5
MDI-TDA	+	5

(-) Insoluble; (±) Partial soluble when heating; (+) Soluble when heating; (++) Good soluble at room temperature

Table 4.18 The solubility of HMDI-based metal-containing copolyureas and reference polyureas

Polymers	DMF	Maximum solubility (mg)/ DMSO 1 mL
ZnSalOMe$_2$trien-HMDI	-	-
NiSalOMe$_2$trien-HMDI	-	-
ZnSalOMe$_2$trien-HMDI-HMDA	-	-
ZnSalOMe$_2$trien-HMDI-DAP	-	-
ZnSalOMe$_2$trien-HMDI-XDA	++	439
ZnSalOMe$_2$trien-HMDI-TDA	++	412
NiSalOMe$_2$trien-HMDI-HMDA	-	-
NiSalOMe$_2$trien-HMDI-DAP	-	-
NiSalOMe$_2$trien-HMDI-XDA	++	24
NiSalOMe$_2$trien-HMDI-TDA	++	95
HMDI-HMDA	-	-
HMDI-DAP	-	-
HMDI-XDA	-	-
HMDI-TDA	-	-

(-) Insoluble; (±) Partial soluble when heating; (+) Soluble when heating; (++) Good soluble at room temperature

The maximum amount of each polymer that was able to dissolve in 1 mL of DMSO was determined as shown in Tables 4.17 and 4.18. For MDI-based metal-containing coPUs, the data showed that most nickel-containing coPUs showed higher solubility than zinc-containing coPUs. In the case of HMDI-based metal-containing coPUs, zinc-containing coPUs showed higher solubility than nickel-containing coPUs. HMDI-based metal-containing coPUs showed lower solubility than MDI-based metal-containing PUUs because they were partially crystalline in nature from the folding of the hexamethylene groups [35-38]. The comparison between metal-containing coPUs synthesized from the same metal complex and diisocyanate showed that TDA-based metal-containing coPUs had better solubility than XDA-, DAP-, and HMDA-based polymers. This might be because TDA has flexible ether bonds. Metal-containing coPUs exhibited lower solubility than metal-containing PUUs because they contain more hydrogen bonding between N-H and C=O group (Figure 4.40).

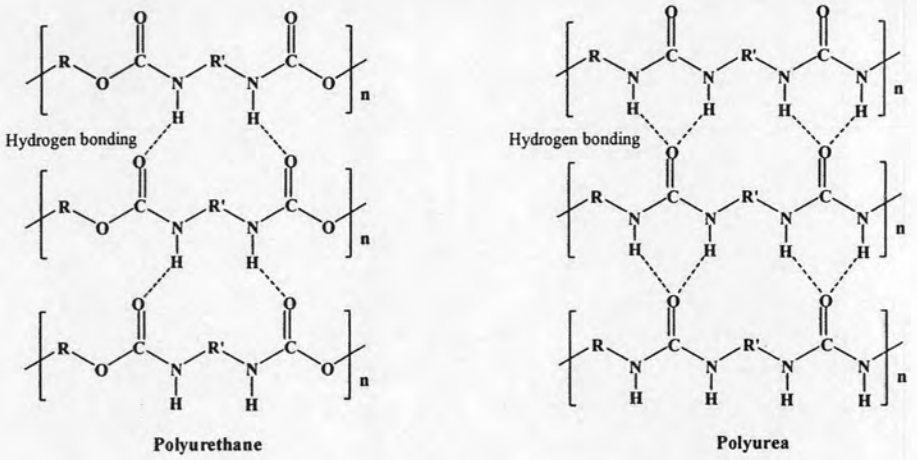

Figure 4.40 Hydrogen bonding in polyurethane and polyurea

Most of metal-containing coPUs was more soluble in DMSO as compared to metal-containing polyureas. These results were comfirmed with XRD data of the polymers.

4.4.2.4 Inherent viscosity

The inherent viscosity of metal-containing coPUs and reference polyureas was measured at a concentration 0.5g/ 100 mL in DMSO 40°C. The viscosity data are shown in Tables 4.19 and 4.20.

Table 4.19 Inherent viscosity of MDI-based metal-containing copolyureas and reference polyureas

Polymers	η_{inh} (dL/g)
ZnSalOMe$_2$trien-MDI-HMDA	-
ZnSalOMe$_2$trien-MDI-DAP	0.0823
ZnSalOMe$_2$trien-MDI-XDA	0.0857
ZnSalOMe$_2$trien-MDI-TDA	0.0909
NiSalOMe$_2$trien-MDI-HMDA	-
NiSalOMe$_2$trien-MDI-DAP	0.0941
NiSalOMe$_2$trien-MDI-XDA	0.0791
NiSalOMe$_2$trien-MDI-TDA	0.0947
MDI-HMDA	0.0765
MDI-DAP	0.0995
MDI-XDA	0.1204
MDI-TDA	0.0942

Table 4.20 Inherent viscosity of HMDI-based metal-containing copolyureas and reference polyureas

Polymers	η_{inh} (dL/g)
ZnSalOMe$_2$trien-HMDI-HMDA	-
ZnSalOMe$_2$trien-HMDI-DAP	-
ZnSalOMe$_2$trien-HMDI-XDA	0.0852
ZnSalOMe$_2$trien-HMDI-TDA	0.0830
NiSalOMe$_2$trien-HMDI-HMDA	-
NiSalOMe$_2$trien-HMDI-DAP	-
NiSalOMe$_2$trien-HMDI-XDA	-
NiSalOMe$_2$trien-HMDI-TDA	-
HMDI-HMDA	-
HMDI-DAP	-
HMDI-XDA	-
HMDI-TDA	-

The data showed that the inherent viscosity of the metal-containing coPUs was found to be in the range between 0.0791-0.0947 dl/g. The viscosity of metal-containing coPUs was slightly lower than those reference polyureas without metal complexes in both Zn and Ni series.

4.4.2.5 X-ray diffraction

Figure 4.41 showed the XRD patterns of ZnSalOMe$_2$trien-MDI-XDA and NiSalOMe$_2$trien-MDI-XDA. Both of them showed broad peaks and therefore they were considered to be amorphous in nature. The amorphous of polymers is supported by the solubility test of polymers that they showed good solubility in DMF and DMSO while metal-containing polyureas were crystalline and therefore they had poor solubility in DMSO.

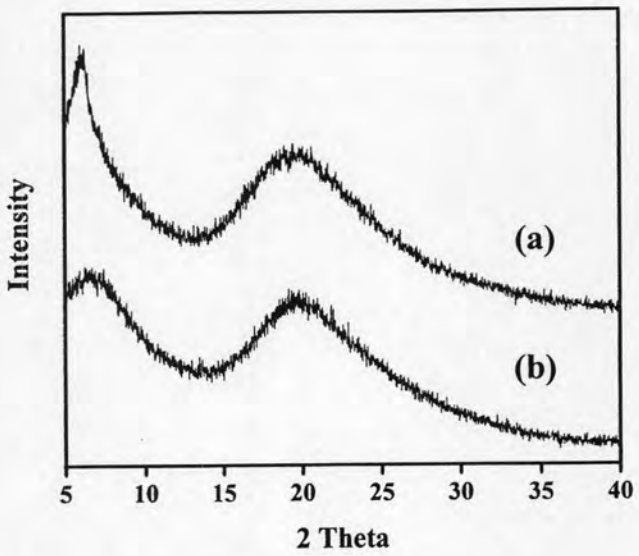

Figure 4.41 XRD patterns of (a) ZnSalOMe$_2$trien-MDI-XDA;
(b) NiSalOMe$_2$trien-MDI-XDA

4.4.2.6 Thermogravimetric analysis and flame retardancy

4.4.2.6.1 MSalOMe$_2$trien-MDI-diamines coPUs

Most zinc-containing coPUs based on MDI had slightly less T_5 and char yields at 600°C than their corresponding ZnSalOMe$_2$trien-MDI, except for ZnSalOMe$_2$trien-MDI-DAP which had higher char yield than ZnSalOMe$_2$trien-MDI (Table 4.22). For MDI-based nickel-containing coPUs, their T_5 and char yield were higher than those of NiSalOMe$_2$trien-MDI. Comparing between zinc- and nickel-containing coPUs, the TGA results showed that zinc-containing coPUs had higher T_5 but lower char yield than nickel-containing coPUs. The presence of different diamine groups in the polymer chain did not have much effect on T_5 and char yields of polymers (Figures 4.42-4.43). Metal-containing coPUs based on DAP showed highest char yields in the range 53-54% from the starting weight because of the diphenylene ring. Most metal-containing coPUs showed lower T_5 than their corresponding reference polyureas synthesized without metal complexes. The char yield at 600°C of HMDA- and TDA-based reference polyureas were 19 and 21% from starting weight, respectively, which were lower than their corresponding metal-containing copolyureas.

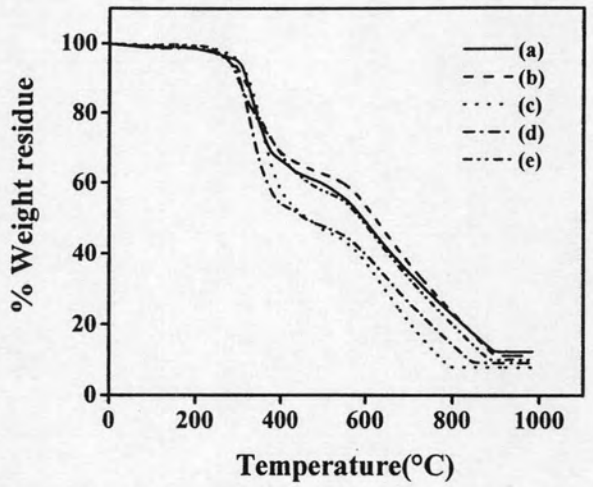

Figure 4.42 TGA thermograms of (a) ZnSalOMe$_2$trien-MDI; (b) ZnSalOMe$_2$trien-MDI-DA; (c) ZnSalOMe$_2$trien-MDI-HMDA; (d) ZnSalOMe$_2$trien-MDI-TDA; (e) ZnSalOMe$_2$trien-MDI-XDA

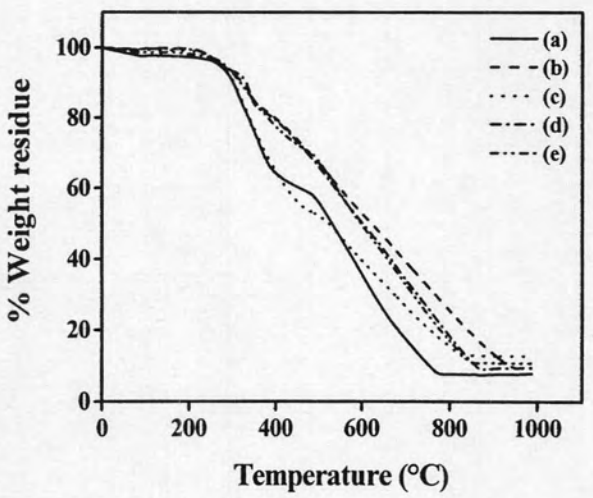

Figure 4.43 TGA thermograms of (a) NiSalOMe$_2$trien-MDI; (b) NiSalOMe$_2$trien-MDI-DA; (c) NiSalOMe$_2$trien-MDI-HMDA; (d) NiSalOMe$_2$trien-MDI-TDA; (e) NiSalOMe$_2$trien-MDI-XDA

Table 4.21 TGA data of MDI-based metal-containing polyureas, copolyureas and reference polyureas

Polymer	T_5 (°C)	Weight loss (%) at different temperature (°C)			LOI
		300	600	800	
ZnSalOMe$_2$trien-MDI	295	6	51	77	27
NiSalOMe$_2$trien-MDI	268	10	64	92	21
ZnSalOMe$_2$trien-MDI-HMDA	297	5	62	92	21
NiSalOMe$_2$trien-MDI-HMDA	273	10	60	85	24
MDI-HMDA	284	7	81	97	19
ZnSalOMe$_2$trien-MDI-DAP	282	8	46	77	27
NiSalOMe$_2$trien-MDI-DAP	272	8	47	75	28
MDI-DAP	321	3	42	77	27
ZnSalOMe$_2$trien-MDI-XDA	275	11	52	80	26
NiSalOMe$_2$trien-MDI-XDA	281	8	50	83	24
MDI-XDA	303	5	45	71	29
ZnSalOMe$_2$trien-MDI-TDA	274	10	60	86	21
NiSalOMe$_2$trien-MDI-TDA	275	7	50	82	25
MDI-TDA	324	2	79	98	18

4.4.2.6.2 MSalOMe$_2$trien-HMDI-diamines coPUs

T_5 of HMDI-based metal-containing coPUs (Table 4.23) were in the range 255-277°C which were lower than that of their corresponding MSalOMe$_2$trien-HMDI. Char yields at 600°C of zinc- and nickel-containing coPUs based on HMDI were not affected by having different diamines in the polymer backbone (Figures 4.44-4.45). They were in the range 37-45% of starting weight. Comparing between metal-containing coPUs and metal-containing polyureas based on HMDI, the presence of diamines did not have the effect on their char yields. HMDI-based zinc-containing coPUs showed slightly higher char yields than their corresponding nickel-containing coPUs. HMDI-based metal-containing coPUs exhibited lower char yields than MDI-based metal-containing coPUs because of the present of aromatic ring in MDI. Most metal-containing coPUs showed lower decomposition rate but higher char yield than reference polyurethanes synthesized without metal complexes.

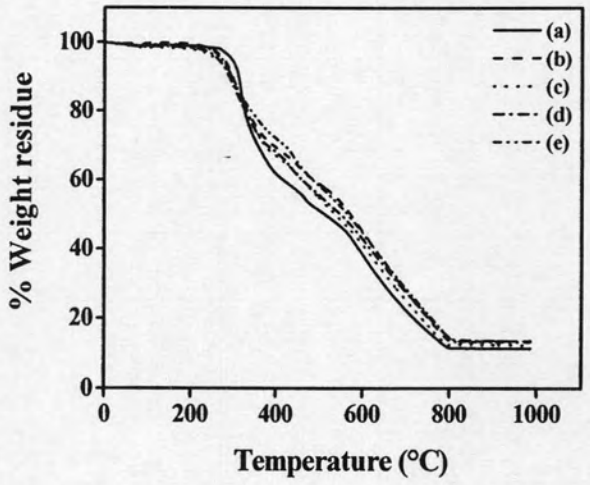

Figure 4.44 TGA thermograms of (a) ZnSalOMe$_2$trien-HMDI; (b) ZnSalOMe$_2$trien-HMDI-DAP; (c) ZnSalOMe$_2$trien-HMDI-HMDA; (d) ZnSalOMe$_2$trien-HMDI-TDA; (e) ZnSalOMe$_2$trien-HMDI-XDA

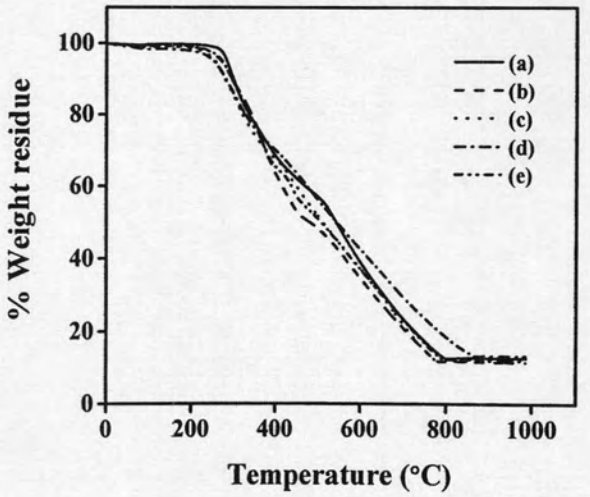

Figure 4.45 TGA thermograms of (a) NiSalOMe$_2$trien-HMDI; (b) NiSalOMe$_2$trien-HMDI-DA; (c) NiSalOMe$_2$trien-HMDI-HMDA; (d) NiSalOMe$_2$trien-HMDI-TDA; (e) NiSalOMe$_2$trien-HMDI-XDA

Table 4.22 TGA data of HMDI-based metal-containing polyureas, copolyureas and reference polyureas

Polymer	T_5	Weight loss (%) at different temperature (°C)			LOI
	(°C)	300	600	800	
ZnSalOMe$_2$trien-HMDI	294	6	62	89	22
NiSalOMe$_2$trien-HMDI	283	11	61	87	23
ZnSalOMe$_2$trien-HMDI-HMDA	260	13	59	87	23
NiSalOMe$_2$trien-HMDI-HMDA	255	15	63	88	22
HMDI-HMDA	306	5	91	98	18
ZnSalOMe$_2$trien-HMDI-DAP	275	11	55	87	23
NiSalOMe$_2$trien-HMDI-DAP	277	9	61	86	23
HMDI-DAP	214	3	76	98	18
ZnSalOMe$_2$trien-HMDI-XDA	272	12	55	86	23
NiSalOMe$_2$trien-HMDI-XDA	272	11	63	88	22
HMDI-XDA	312	4	72	98	18
ZnSalOMe$_2$trien-HMDI-TDA	263	13	57	85	24
NiSalOMe$_2$trien-HMDI-TDA	252	14	57	82	25
HMDI-TDA	329	2	94	98	18

Flame retardant properties of metal-containing coPUs were compared from their limiting oxygen index (LOI) values (Table 4.23) and were calculated from char yield by Van Krevelen and Hoftyzer equation [39-41].

Van Krevelen and Hoftyzer equation: LOI = 17.5 + 0.4CR

Where CR = char yield at 800°C

All metal-containing coPUs showed the same LOI value in the range 22-25. The metal-containing coPUs based on MDI showed slightly higher flame retardancy than those derived from HMDI because of the presence of aromatic rings in the main chain of polymers. The LOI values of metal-containing coPUs based on MDI and two aromatic diamines, DAP and XDA, were higher than those of HMDA- and TDA-based polymers.